NUREG/CR-1651
BNL-NUREG-51258

CONSTITUTIVE RELATIONS IN TRAC-P1A

UPENDRA S. ROHATGI AND PRADIP SAHA

DO NOT MICROFILM
COVER

MASTER

Date Published: August 1980

NUCLEAR SAFETY PROGRAMS
DEPARTMENT OF NUCLEAR ENERGY, BROOKHAVEN NATIONAL LABORATORY
UPTON, NEW YORK 11973

Prepared for the U.S. Nuclear Regulatory Commission
Office of Nuclear Regulatory Research
Contract No. DE-AC02-76CH00016

DISCLAIMER

NUREG/CR-1651
BNL-NUREG-51258
AN, R-4

CONSTITUTIVE RELATIONS IN TRAC-P1A*

UPENDRA S. ROHATGI AND PRADIP SAHA

NUREG/CR--1651

TI85 015956

Date Published: August 1980

NUCLEAR SAFETY PROGRAMS
DEPARTMENT OF NUCLEAR ENERGY, BROOKHAVEN NATIONAL LABORATORY
UPTON, NEW YORK 11973

*This document has been prepared to answer the questions concerning the Basic Thermal-Hydraulic Models in TRAC-PIA code as requested by Dr. S. Fabic of NRC. The report follows the format of the questions which are attached hereto for completeness.

PREPARED FOR THE U.S. NUCLEAR REGULATORY COMMISSION
OFFICE OF NUCLEAR REGULATORY RESEARCH
UNDER CONTRACT NO. DE-AC02-76CH00016
FIN A-3215

Available from
GPO Sales Program
Division of Technical Information and Document Control
U.S. Nuclear Regulatory Commission
Washington, D.C. 20555
and
National Technical Information Service
Springfield, Virginia 22161

PREFACE

The purpose of this document is to describe the basic thermal-hydraulic models and correlations that are in the TRAC-P1A code, as released in March 1979. It is divided into two parts, A and B. Part A describes the models in the three-dimensional Vessel module of TRAC, whereas Part B focuses on the loop components that are treated by one-dimensional formulations. The report follows the format of the questions prepared by the Analysis Development Branch of USNRC and the questionnaire has been attached to this document for completeness.

Concerted efforts have been made in understanding the present models in TRAC-P1A by going through the FORTRAN listing of the code. Some discrepancies between the code and the TRAC-P1A manual have been found. These are pointed out in this document. Efforts have also been made to check the TRAC references for the range of applicability of the models and correlations used in the code.

Finally, the authors would like to thank Dr. D. R. Liles and Dr. D. A. Mandell of LASL for a number of helpful telephone conversations on the basic models in TRAC. Suggestions and comments of Dr. O. C. Jones, Jr. and Dr. W. Wulff of BNL, of Dr. N. Zuber of NRC, and of the other members of the Advanced Code Review Group are also appreciated. Typing of Ms. T. Rowland and Mrs. J. V. Muller is also appreciated.

THIS PAGE

WAS INTENTIONALLY

LEFT BLANK

TABLE OF CONTENTS

LIST OF FIGURES

LIST OF TABLES

STANDARD NOMENCLATURE

Independent Variables

r	Radial coordinates in cylindrical geometry
t	Time
θ	Azimuthal coordinate in cylindrical geometry
z	Axial coordinate in cylindrical geometry

Other Variables

A	Area
C	Shear or friction coefficient in two-fluid equations
c_p	Specific heat at constant pressure
c_v	Specific heat at constant volume
D	Diameter
e	Specific internal energy
E	Mass fraction of entrained liquid
f	Friction factor in drift-flux equations
FA	Flow area
g_c	Acceleration due to gravity
G	Mass flux (ρV)
h	Specific enthalpy or heat transfer coefficient
h_{fg}	Latent heat of vaporization
k	Thermal conductivity, form loss coefficient, or pipe roughness
K	Wall shear coefficient in drift-flux equations
m	Mass
Nu	Nusselt number
p	Pressure
Pr	Prandtl number
q	Heat generation rate
q''	Heat flux
q'''	Volumetric heat generation rate
R	Radius
Re	Reynolds number
T	Temperature

Other Variables (continued)

V	Velocity
vol	Hydrodynamic cell volume
We	Weber number
X	Axial coordinate in 1-D formulation
x	Quality
α	Vapor volume fraction
Γ_v	Net volumetric vapor production rate due to phase change
δ	Mean-fuel surface roughness
Δ	Increment
ε	Emissivity
μ	Viscosity
ρ	Microscopic density
σ	Surface tension or Stefan-Boltzmann constant
τ	Shear stress
Φ^2	Two-phase friction factor multiplier
ω	Angular Velocity

Subscripts

b	Bubble
c	Cladding
d	Droplet
f	Fuel or friction
g or v	Vapor (gas) field
h	Hydraulic
i	Interface (liquid-vapor) quantity or one-dimensional cell index in heat transfer equations
j	One-dimensional cell index in hydrodynamics equations
ℓ	Liquid field
ℓg	Liquid to vapor
m	Mixture quantities
mw	Metal-water reaction
qf	Quench front
r	Relative
r,θ,z	Cylindrical coordinate directions

Attachment I

List of Questions Concerning the Basic Thermo-Hydraulic Models in TRAC code.

Part A: Liquid/Vapor and Fluid/Solids Interactions in Vessel Module of TRAC.

Part B: Liquid/Vapor and Fluid/Solids Interactions in other System Components.

Detailed answers are requested to all questions that are relevant to the TRAC-P1A code released to the public during the first half of calendar yeat 1979.

In future answers to similar questions, related to future versions of TRAC, please indicate either "no change" or give details of the changes made.

The Advanced Code Review Group may recommend changes to this questionnaire since not all of the listed effects may be thought important enough to require their consideration in the systems code. However, in the first iteration, on TRAC-P1A, answers to all questions are urged.

At the end of each section in Parts A and B, describe, wherever possible, the data base used in formulating models and assigning coefficients. Indicate the range of applicability and discuss limitations and uncertainties.

A. LIQUID/VAPOR AND FLUID/SOLIDS INTERACTIONS IF VESSEL MODULE OF TRAC.....

1.0 Flow Regime Recognition Criteria.

1.1 Describe General Criteria

1.2 Describe specific criteria, if such exist in code, for:

Vessel Region	Regime of LOCA (Blowdown, Refill, Reflood)	Very low flows as in Small Breaks
Downcomer		
Lower Plenum		
Core		
Upper Plenum		

Enter "No" when specific criteria are not used. Otherwise indicate subsection number where the criteria are described in this document.

1.3 Describe how transition is handled in the code between adjacent flow regimes.

2.0 Liquid/Vapor Mass Exchange Models. Also Source/Sink Terms for Non-Condensible Gas.

2.1 Describe (a) Evaporation Model(s)

(b) Condensation Model(s)

2.2 How are they related to general flow regime criteria?

2.3 How are they related to specific flow regime criteria indicated in Table on pg. 1, or any other criteria?

2.4 How related to flow magnitude (turbulence level)?

2.5 Describe models for source and sink terms for noncondensible gas, where applicable.

2.6 Do mass exchange models account for the presence of (a) solids (nucleation sites), (b) noncondensible gas, and how?

2.7 Are nucleation delays or superheat thresholds handled?

3.0 Liquid/Vapor Momentum Exchange Models

3.1 Describe the models for momentum exchange at liquid/vapor or liquid/gas interfaces, as functions of generalized flow regime map.

3.2 As functions of specific flow regime criteria related to vessel region and/or regime of LOCA and/or very low flows (small break).

3.3 Are they functions of flow orientation (upflow, downflow, lateral and/or inclined flow)? If so give details.

4.0 Solids (Walls or Embedded Hardware) to Fluid Momentum Exchange Models

4.1 Describe models as function of generalized flow regime map.

4.2 Also as functions of specialized flow regime criteria if such are employed:

4.3 Give details of treatment for inclined and lateral flow in reactor core and in Upper Plenum, as functions of flow regime. How are the form losses calculated and how are friction losses calculated in single and two-phase flow regimes?

4.4 How are two-phase pressure drops calculated for abrupt changes in flow area (e.g. at core inlet and outlet support plates, core grids, junctions between nozzles and vessel plena and/or downcomer)?

4.5 If more than one phase (or fluid component) are adjacent to solids within the same computational cell, how is the momentum exchange partitioned?

4.6 Is the momentum exchange a function of solid's surface temperature (that indicates whether the solid can be wetted by the liquid or not)?

5.0 Liquid Entrainment and Deposition

Describe the models if such are used in the code and indicate dependance on flow orientation, magnitude of absolute and/or relative flow (between liquid and steam), flow path geometry, temperatures, pressure, etc.

6.0 Counter-Current Flow Limitation and Liquid Fallback at the Core Support Plates

Give modeling details and, if special, empirically based models are used describe the criteria which trigger their use.

7.0 Energy Transfer Between Liquid and Vapor Fields

7.1 Describe the models used to obtain heat flux to, or from, the bulk fluid and the liquid/vapor interface within the computational cell.

7.2 Indicate how these are related to the mass exchange model(s).

7.3 Indicate how the energy transport models, at interfaces, are related to generalized and/or specialized flow regimes.

8.0 Energy Transfer Between Solids (Walls, Internal Structure, Fuel Rods) and Fluid

8.1 Describe the models and relate them to flow and heat transfer regimes.

8.2 List all heat transfer regimes considered for the reactor core and indicate if all, or a selected subgroup, are employed for treatment of heat transfer to and from the walls and internal structures.

8.3 Define selection criteria used to identify each heat transfer regime.

8.4 Describe heat transfer correlations for each regime, indicating dependance on flow and fluid state parameters.

8.5 How is heat transfer handled for flow (component) perpendicular to fuel rods?

8.6 In flow regimes where both liquid and vapor are adjacent to solids in the same computational cell, indicate how the energy is partitioned. Such situations occur, for example, when liquid, or froth, interface is traversing any computational cell containing walls or solid structures.

8.7 Describe model(s) for quench front propagation and indicate if multiple (two or more) quench fronts can be monitored.

8.8 How does the quench front propagation model handle flow reversals and the effects of grid spacers?

B. LIQUID/VAPOR AND FLUID/SOLID INTERACTIONS IN LOOP COMPONENTS OF TRAC....

1.0 Flow Regime Recognition Criteria

1.1 Describe general criteria

1.2 Describe specific criteria, if such exist, for steam generator, pressurizer, horizontal vs. vertical pipes, etc., and if functions of LOCA regimes. Is special treatment being used, and where, for very small break LOCA and for natural circulation (of Reflux Boiler type).

1.3 How are transitions handled between flow regimes?

2.0 Liquid/Vapor Mass Exchange Models and Noncondensible Gas Source/Sink Terms

2.1 Describe (a) Evaporation model

(b) Condensation model

2.2 How are the evaporation and condensation models related to the flow regime criteria and is special treatment being used for individual loop components? If so, please give details.

2.3 Are turbulence effects modeled (either directly or indirectly)? Any other flow magnitude effects?

2.4 Is the presence of embedded solids and walls taken into account and how?

2.5 Are the effects of noncondensible gas treated and how?

2.6 Is nucleation delay (or incipient superheat) handled, and how?

2.7 How are the mass exchange models related to the interfacial energy exchange models and, where appropriate, to solids/fluid energy exchange models?

2.8 How are sources and sinks for noncondensible gas described (for example, for gas coming out of solution or being forced back into solution)?

3.0 Liquid/Vapor Momentum Exchange Models

3.1 Describe the model(s) and indicate which is used in what flow regime and whether special treatment is given to some loop components.

3.2 Are the models functions of flow orientation (upflow, downflow, horizontal flow, and counter-current flow) and, if so, give details?

3.3 What steps are taken to prevent smearing of the liquid/vapor interface in analysis of small breaks (to assure that (a) proper heat transfer regimes are handled and proper fluid fluxed to nozzles)?

4.0 Walls-to-Fluid Momentum Exchange Models

4.1 Describe models as functions of flow regimes and indicate if any special treatment is given in particular loop components.

4.2 Describe treatment of two-phase flow pressure drop for flow area expansion, contraction, orifices.

4.3 How is the void fraction distribution handled for flow through tees, and also for flow into steam generator tubes, in steady and transient flow conditions? If these effects are handled through liquid/vapor momentum exchange models (or through vapor drift models) please indicate these answers in Section 3.0.

4.4 If more than one phase are adjacent to walls within the same computational cell (as during the rise or fall of liquid level or in stratified flow in the horizontal pipes), how is the wall-to-fluid momentum exchange partitioned? This particular question is pertinent to the two-fluid formulation.

5.0 Liquid Entrainment and Deposition Models

Is entrainment and deposition of liquid modeled in the code (for loop components) and, if so, how?

6.0 CCFL

Are any special models being used to account for counter-current flow limitation? If so, give details.

7.0 Models for Energy Transfer Between Liquid and Vapor

7.1 Describe the models and indicate how are they related to flow regimes?

7.2 How are they related to interfacial mass transfer models?

8.0 Energy Transfer Between Solids (Walls) and Fluid

8.1 Describe the models and relate them to flow and heat transfer regimes.

8.2 List all heat transfer regimes considered in (a) Steam generator primary and the secondary side, (b) other loop components.

8.3 Define selection criteria used to identify each heat transfer regime including the S.G. secondary side.

8.4 Describe the heat transfer correlations that are different from those shown in Part A. Otherwise indicate that they are the same.

8.5 In flow regimes where both liquid and vapor are adjacent to solids in the same computational cell, indicate how the energy is partitioned.

INTRODUCTION

Brookhaven National Laboratory (BNL) is involved in an ongoing task of reviewing and assessing various versions of the TRAC code as they are released to the public. This task, in principle, should consist of assessing the conservation laws, the intrinsic constitutive relations (material properties), the extrinsic constitutive laws (i.e., the models and correlations for the transfer laws), the numerical techniques and the coding quality assurance. However, the emphasis at BNL has been to assess the extrinsic constitutive laws by checking the formulations as coded in TRAC and by comparing the TRAC predictions with the various basic and separate-effects tests.

This report has been prepared in response to a two part (A & B) questionnaire provided by the Analysis Development Branch of USNRC. The list of questions has been attached at the beginning of this report. The first part (i.e., Part A) deals with the three dimensional, two-fluid formulation for the vessel, while the second part (Part B) deals with the one-dimensional drift flux formulation for the remaining loop components. Each of these parts has been further divided into eight sections, which describe various topics such as flow regime recognition criteria, liquid/vapor mass, momentum and energy exchange, liquid entrainment and deposition, counter-current flow limitation and finally, solid/fluid momentum and energy exchange.

This report is in the form of answers to the specific questions on these eight topics, and it should be read along with these questions. The emphasis here has been to describe what exists in the TRAC-P1A documentation and the code, and to point out any differences between them. Furthermore, the models and the correlations in TRAC-P1A have also been checked with the original references, wherever possible, to indicate any discrepancy in their use and also to provide the limitation of these models and the data base used to develop them. The authors have also provided their opinion on these models wherever deemed necessary.

Therefore, this report will not only supplement the TRAC-P1A documentation for describing the models in the code but can also be used as a limited review of the constitutive relationships used in the two-fluid and the drift-flux formulations of TRAC-P1A.

A. LIQUID/VAPOR AND FLUID/SOLID INTERACTIONS IN THE VESSEL MODULE OF TRAC

The vessel module has a two-fluid, three-dimensional formulation. The balance equations consist of mixture and vapor mass balances, mixture and vapor energy balances and the momentum conservation for the liquid and the vapor phases. These balance equations require descriptions of relative velocity, V_r, vapor generation rate, Γ_v, interfacial drag, interfacial heat and mass transfer, interfacial velocities, interfacial area, wall heat transfer for the liquid and the vapor and corresponding wetted areas. All these descriptions depend on flow regimes.

1.0 Flow Regime Recognition Criteria

1.1 In the vessel module, TRAC uses a very simple flow regime map, which is based only on cell centered void fraction. This map is shown in Figure A.1. This map has bubbly flow, slug flow and annular or annular mist flows. LASL refers to a BNL Quarterly report (Lekach, 1975) for this map, however it is somewhat different from the reference.

1.2 There is no specific flow regime criterion for different components such as downcomer, lower plenum, core, and upper plenum. These are treated as part of the vessel module with internals. However, there is a special flow regime criterion for reflood conditions, and it has been described in Section A.8.1.

1.3 The TRAC documentation (TRAC-P1A, 1979) identifies the use of the flow regime map given in Figure A.1 for computing interfacial heat transfer. However, TRAC uses a somewhat different map, which is shown in Figure A.2. This map has a transition region between the bubbly and slug flow regimes in mass flux direction and another one between slug or bubbly flow and annular mist regimes. In all these transition regions, a linear interpolation function based on either mass flux or void fraction is used. TRAC-P1A documentation defines bubbly to slug flow transition at $\alpha = 0.25$, while in the TRAC-P1A code, the transition takes place at $\alpha = 0.3$.

2.0 Liquid/Vapor Mass Exchange Model

2.1 Mass Transfer between the phases takes place at the interface and is related to heat transfer rates there.

$$\Gamma_v = \frac{-q_{ig} - q_{i\ell}}{h_{sg} - h_{s\ell}} \qquad (A.2.1)$$

Here Γ_v is the vapor generation rate, q_{ig} and $q_{i\ell}$ are the rate of heat transfer per unit volume from the interface to the vapor and from the interface to the liquid, respectively; while h_{sg} and $h_{s\ell}$ are saturation enthalpies for vapor and liquid, respectively.

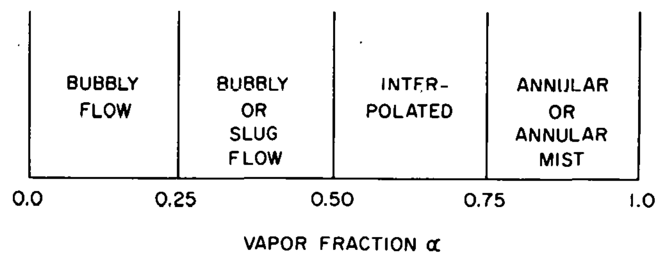

Figure A.1. Flow Regime Map

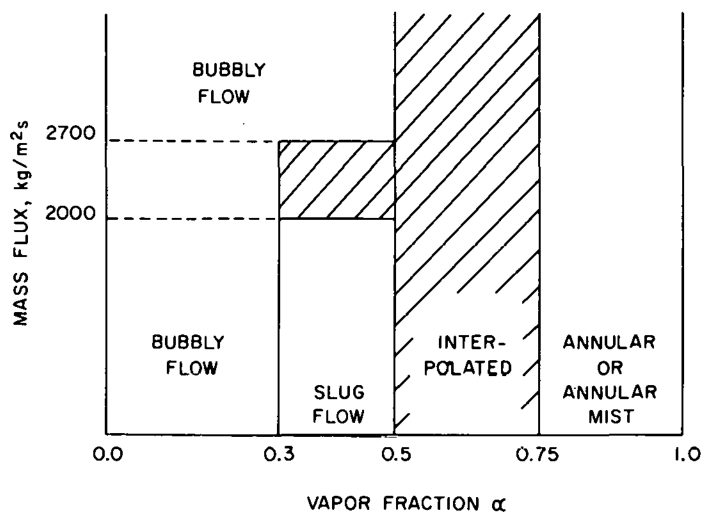

Figure A.2. Flow Regime Map (Cross hatched regions are transition zones)

Also,

$$q_{i\ell} = h_{i\ell} A_i (T_s - T_\ell)/vol \qquad (A.2.2)$$

$$q_{ig} = h_{ig} A_i (T_s - T_g)/vol \qquad (A.2.3)$$

Here A_i is the interfacial area, $h_{i\ell}$ and h_{ig} are the heat transfer coefficients on the liquid and the gas side of the interface, and vol is the fluid volume of the cell.

2.1.1 Bubbly Flow

The flow regime map as shown in Figure A.2 is used to provide interfacial area and the heat transfer coefficient for the liquid side. When the cell center void fraction is less than or equal to 0.30 or if the mass flux is greater than 2700 kg/m^2s and void fraction is less than 0.50, a bubbly flow exists. In this flow regime, it is assumed that all the bubbles are of the same size and their diameter can be obtained from a critical Weber number. It is stated in the TRAC documentation that the results are not very sensitive to this Weber number and a critical Weber number of 50 is used in the code.

$$We_b = \frac{\rho_\ell V_r^2 D_b}{\sigma} = 50 \qquad (A.2.4)$$

Here V_r is the relative velocity between the vapor and the liquid. This relative velocity is computed in the code by taking the differences of the magnitude of the vapor and liquid phase velocities. However, if V_r is less than 1.0m/s, it is set equal to the larger of 1.0m/s or one fifth of the magnitude of the liquid velocity*. There seems to be no justification for these steps. D_b and σ are the bubble diameter and the surface tension, respectively. The bubble diameter calculated from the above equation and the void fraction provide the number of bubbles and thus the interfacial area, as shown below:

$$A_i = \frac{6\alpha \, vol \, \rho_\ell V_r^2}{We_b \, \sigma} \qquad (A.2.5)$$

*This constraint has been removed in corrected TRAC-P1A vessel module, but retained in loop components.

The heat transfer coefficient for the liquid side is obtained from the larger of the two expressions given here.

$$Nu = \frac{3}{\pi} \frac{\left(T_\ell - T_s\right) \rho_\ell \, c_{p,\ell}}{\rho_g \, h_{fg}} \tag{A.2.6}$$

$$Nu = 2 \cdot 0 + 0.74 \, Re_b^{0.5} \tag{A.2.7}$$

where

$$Re_b = \frac{\rho_\ell \, V_r \, D_b}{\mu_\ell} \tag{A.2.8}$$

The first of these expressions is obtained from the Plesset-Zwick (1954) bubble growth expression by replacing time in the denominator in terms of bubble radius. However, following this procedure one obtains four times the Nusselt number given in Equation (A.2.6), and the correct expression should be

$$Nu = \frac{12}{\pi} \frac{(T_\ell - T_s) \, \rho_\ell \, c_{p,\ell}}{\rho_g \, h_{fg}} \tag{A.2.9}$$

The TRAC code has this correct expression. However, the $(T_\ell - T_s)$ term in the code is restricted between 1 and 10°K. The second expression (A.2.7) is claimed to be from Lee & Ryley (1968). However, they studied heat transfer between water droplets and superheated steam, and their expression is given as

$$Nu = 2 + 0.74 \, Re^{0.5} \, Pr^{0.33} \tag{A.2.10}$$

This expression was obtained from 92 tests on water droplets with the following conditions:

Initial nominal diameter of droplets	230 - 1126 μm
Droplet Reynolds number	64 - 250
Degrees of superheat	3 - 38°C
Steam pressure	1.013 - 1.992 bar
Steam velocity	2.68 - 11.94 m/s

The Prandtl number effect of the surrounding medium has apparently been neglected in Equation (A.2.7). This assumption is justified since the Prandtl number of water at high temperature (> 150°C) is close to 1.0.

The interfacial mass transfer also requires the heat transfer coefficient at the interface on the vapor side. In the bubbly and slug flow regimes, the heat transfer coefficient is assumed to be a constant.

$$h_{ig} = 10^4 \text{ W/m}^2\text{-°K}$$

2.1.2 Slug Flow

When the cell center void fraction is between 0.3 to 0.5, and the cell average mass flux is less than 2000 kg/m^2s, the flow is in the slug regime. In this regime it is assumed that the void fraction of the mixture in the liquid slug (or the trailing bubble) region varies from 0.3 to 0.2 as the total mixture void fraction varies from 0.3 to 0.5. That is to say that at α = 0.30, all the voids are in the liquid slug region and a Taylor bubble just starts to form. Whereas, at α = 0.50, only 40% of all the voids are in the liquid slug region and the remaining 60% form the Taylor bubble. Govier & Aziz (1972) on page 402 show the results from the experiments done by Akagawa & Sakaguchi (1966) with air-water vertical flow in a 2.77 cm diameter tube, with superficial velocities for air and water limited to 1.49 m/s and 0.79 m/s, respectively. The authors concluded from their results that the void fraction of the mixture in the liquid slug (or the trailing bubble) region is at most only 10%. The heat transfer coefficient and the interfacial area in the trailing bubbles are computed in the same way as in the bubbly flow regime. While, for the Taylor bubbles, the heat transfer coefficient is computed as for a film on the wall (see Section 2.1.3), and its interfacial area is given by the following expression

$$A_i = 5 \text{ (Vapor Volume in Taylor bubble)}/D_h$$

However, in the intermediate range of mass flux between 2700 kg/m^2s and 2000 kg/m^2s, a linear interpolation between the slug regime and the bubbly regime heat transfer rates is used.

2.1.3 Annular/Annular Mist Flow

The annular flow or annular mist flow exists when the void fraction is between 0.75 and 1.0. In this regime the mass fraction of liquid in the form of entrained droplets is computed from the Wallis correlation as given here (see Section A.5 for details).

$$E = 1 - \exp\left(- 0.125 \left(J_g^{\prime} - 1.5\right) \right) \tag{A.2.11}$$

where

$$J_g^{\prime} = 10^4 \alpha \frac{V_g \mu_g}{\sigma} \left(\frac{\rho_g}{\rho_\ell} \right)^{1/2} \tag{A.2.12}$$

and E is the mass fraction of the liquid in droplet form. The remaining liquid is in the form of a film on the wall. The interfacial area is sum of the areas of the film and of the droplets. The droplets are assumed to have the same size and their diameter is obtained from a critical Weber number, in the same way as for the bubbles. However, a critical Weber number of 2 is used. The expressions leading to the heat transfer coefficient on the liquid side of the droplet are

$$D_d = We_d \, \sigma \Big/ \rho_g V_{rd}^2 \tag{A.2.13}$$

$$V_{rd} = 1.4 \, \alpha \left[g \, \sigma \, (\rho_\ell - \rho_g) \Big/ \rho_g^2 \right]^{1/4} \tag{A.2.14}$$

$$h_{i\ell} = 15000 \, k_\ell / D_d \tag{A.2.15}$$

The TRAC-P1A manual does not cite any reference for the above equation.

The interfacial area due to the liquid film is calculated in TRAC-P1A as follows:

$$A_i = (\pi D_h \, \Delta z) \quad (1-E) \cdot \text{Multiplier} \tag{A.2.16}$$

where Δz is the cell length and,

Multiplier = 5.0 for vessel

Multiplier = 500 for loop components

The TRAC-P1A documentation does not give this expression and also does not justify using (1-E) and the multiplier.

The heat transfer coefficient for the liquid film is given as

$$h_{i\ell} = 0.0073\, \rho_\ell\, k_\ell\, V_\ell \,/\, \mu_\ell \tag{A.2.17}$$

There is no reference given for this expression. However, it seems that the expression is obtained from the work of Linehan (1968).

The interfacial heat transfer rate on the liquid side, $q_{i\ell}$, for annular mist flow is then computed from the volume average between the droplet and the film heat transfer coefficients times the corresponding interfacial areas and the temperature differences.

In the annular mist regime, TRAC-P1A computes the heat transfer coefficients on the vapor sides of the liquid-vapor interfaces at the liquid film and at the droplets and volume averages them. The heat transfer coefficient on the vapor side of the droplets is computed from the expression given in Equation (A.2.10). However, for the film it is similar to Equation (A.2.17) and is given by

$$h_{ig} = 0.0073\, \rho_g\, k_g\, V_g \,/\, \mu_g \tag{A.2.18}$$

There is a mistake in the TRAC coding of this expression in one-dimensional components. The code has 0.00073 instead of 0.0073.

2.1.4 Transition Regime

The region of void fraction between 0.50 and 0.75 is a transition region. A linear interpolation function based on void fraction is used between the computed values of interfacial heat transfer coefficient times the interfacial area at $\alpha = 0.5$ and at $\alpha = 0.75$. However, the computation of relative velocity for the purpose of determining the interfacial area in this region seems to be in error.

2.1.5 Condensation Regime

In case of condensation, a film type of model is used to compute $q_{i\ell}$. This means that all the liquid is assumed to be in the film on wall. However, the interfacial area in this case is computed in the code as five times the vertical flow (or cross-sectional) area, i.e.,

$$A_i = (vol/\Delta z) * 5 \qquad (A.2.19)$$

This is not consistent with the film type model assumed for the interfacial heat flux calculation. The TRAC-P1A documentation gives this area as ten times the flow area.

2.1.6 Some General Features

So far we have discussed the interfacial heat transfer rates for various flow regimes and for condensation. The TRAC-P1A code has certain restrictions on these rates which are not documented and apply to all the flow regimes. The heat transfer coefficient times the interfacial area on the vapor side (CHTI) is corrected by an exponential of vapor subcooling.

$$CHTI = CHTI * EXP\ (T_s - T_v)$$

Here vapor subcooling is restricted between 0°C and 7°C. Furthermore, CHTI is set to be at least equal to the cell volume times 10^7. In case of loop components, it has also a lower limit of flow area times 1000. On the other hand, the CHTI is further limited in the vessel by expressions which are functions of time step and old CHTI.

The heat transfer coefficient times the interfacial area on the liquid side (ALV) is in general restricted to be greater than flow area times 1000. However, it is further limited in the vessel by expressions which are functions of time step and old ALV. These restrictions on CHTI and ALV do not seem to have any physical basis.

2.2
&
2.3 Relationship with flow regime has been described in 2.1

2.4 TRAC-P1A accounts for flow magnitude through Reynolds number in heat transfer coefficients at the interface.

2.5 There is no model to account for noncondensible gas.

2.6 The mass exchange models do not account for nucleation sites or noncondensible gas.

2.7 There is no mechanism to handle nucleation delays or superheat thresholds in TRAC-P1A.

3.0 Liquid/Vapor Momentum Exchange Model

3.1 The vessel module is described by two fluid formulations. There are separate momentum balance equations for the liquid and the vapor. The interfacial momentum transfer terms appearing in the vapor and the liquid equations of motion are given here.

$$\frac{C_i \; V_r \mid V_r \mid}{\alpha \; \rho_g} \quad , \quad \frac{C_i \; V_r \mid V_r \mid}{(1-\alpha) \; \rho_\ell} \quad , \tag{A.3.1}$$

where C_i is the shear coefficient and V_r is the relative velocity. The shear coefficient C_i is a function of flow regime as shown in Figure A.2.

3.1.1 Bubbly Flow

When the cell center void fraction is less than 0.30 or the mass flux is greater than 2700 kg/m^2-s with $\alpha < 0.5$, there is bubbly flow. The bubble size and the interfacial area are obtained from the critical Weber number and the cell center void fraction as has been shown in Section A.2.1.

$$D_b = \frac{We_b \; \sigma}{\rho_\ell \; V_r^2} \tag{A.3.2}$$

$$Re_b = \frac{\rho_\ell \; V_r \; D_b}{\mu_\ell} \tag{A.3.3}$$

In TRAC-P1A, the shear coefficient C_i is related to a bubble drag coefficient C_b as

$$C_i = \frac{C_b \; \alpha \; \rho_\ell}{2 \; D_b} \tag{A.3.4}$$

However, this expression should correctly have 3/4 instead of 1/2. Furthermore, here C_b is obtained from the standard formula for a sphere (Govier & Aziz, page 366), except for $Re_b < 0.1$.

$$\begin{aligned} C_b &= 240 && Re_b < 0.1 \\ &= 24/Re_b && 0.10 < Re_b < 2, \; D_b < 0.001\text{m} \\ &= 18.7/Re_b^{\,0.68} && 2 < Re_b < 4.02 \; G_1^{-.214} \end{aligned} \tag{A.3.5}$$

where

$$G_1 = \frac{g\,\mu_\ell^4}{\rho_\ell\,\sigma^3} \qquad (A.3.6)$$

This description of drag coefficient is not continuous at Re = 2. Furthermore, if the bubble Reynolds number increases further, the bubbles will deform and this method of computing the bubble drag coefficient will not be correct. Also, the bubble drag coefficient will be much larger as given by the following expressions (Govier & Aziz, Page 366).

$$C_b = 0.0275\ G_1\ Re_b^4\ ,\quad 4.02\ G_1^{-.214} \le Re_b \le 3.10\ G_1^{-.250} \qquad (A.3.7)$$

$$C_b = 0.82\ G_1^{0.25} Re_b\ ,\quad 3.10\ G_1^{-0.25} \le Re_b \qquad (A.3.8)$$

The TRAC-P1A has only expressions (A.3.5) which are consistent with the spherical bubbles. Furthermore, the code applies these expressions beyond the upper limits on the bubble diameter and the Reynolds number as given in (A.3.5). However, it does have the lower constraint on C_b.

$$C_b > 0.44 \qquad (A.3.9)$$

3.1.2 Slug Flow

When the mass flux is less than 2000 kg/m^2s and the cell center void fraction is between 0.30 and 0.50, the flow is in the slug regime. In this regime, the void fraction of the mixture in the trailing bubble region is assumed to be between 20% and 30% (see Section A.2.1). The interfacial shear on these bubbles is computed as is done for the bubbly flow regime. The remaining vapor is in the form of a Taylor bubble and a drag coefficient of 0.44 is assumed for it. The TRAC-P1A documentation states that the interfacial drag in the slug regime is volume averaged between this Taylor bubble and the trailing bubbles. However, the contribution of the Taylor bubble to the interfacial shear stress could not be found in the code.

3.1.3 Annular/Annular Mist Flow

When the cell center void fraction is greater than 0.75, the flow is either annular or annular mist flow. The amount of the entrained liquid which forms the mist is computed by Wallis's entrainment correlation, which has probably been obtained by curve fitting the tube data described in Section A.5. The droplet size is obtained as explained in Section A.2.1. The expressions leading to the interfacial shear coefficient on droplets are the same as in (A.3.5) and given as follows:

$$Re_d = \frac{\rho_g V_{rd} D_d}{\mu_g} \tag{A.3.10}$$

$$\begin{aligned} C_d &= 240 & Re_d &< 0.1 \\ &= 24/Re_d & 0.1 \le Re_d &\le 2 \\ &= 18.7/Re_d^{0.68} & Re_d &> 2 \end{aligned} \tag{A.3.11}$$

The drag coefficient in Equation A.3.11 is not continuous at $Re_d = 2$ and jumps from 12 to 11.67.

The shear coefficient on the liquid film is computed from the following expression

$$C_i = 0.01 \, (1+300 \, (1-\alpha) \, (1-E)) \tag{A.3.12}$$

The expression is at variance with Wallis' (1970) correlation for the annular film flow and the correct expression is given here as

$$C_i = 0.01 \, (1+75 \, (1-\alpha) \, (1-E)) \tag{A.3.13}$$

This correlation was developed from the data obtained from air-water flow in tubes up to 7.62 cm in diameter. The liquid film on the wall was thin ($\delta/D < 0.04$).

The net interfacial shear stress in annular/annular mist flow regime is computed by volume averaging shear stress on the droplets and on the film.

3.2 The effect of flow regime on the liquid vapor momentum exchange has been shown in previous sections. Furthermore, there is no special modelling for it for small breaks.

TRAC-P1A computes interfacial shear coefficients for the axial direction which is then used to find shear coefficients in the radial and the azimuthal directions. This is shown in Section 3.3.

3.3 The TRAC formulation requires interfacial shear stresses in axial, radial and azimuthal directions. The axial and radial component of interfacial shear are assumed to be the same and are computed on the basis of axial conditions, and the flow regime map as shown in Figure A.2. In this calculation, the magnitude of the fluid velocity is used to compute the Reynolds number.

However, the azimuthal component is treated slightly differently. First, the Reynolds number is based on azimuthal component of the velocity, and secondly the flow regime map in this direction has the bubbly flow regime up to $\alpha = 0.5$, instead of the slug regime between $\alpha = 0.30$ and $\alpha = 0.5$. TRAC-P1A computes void fractions at the cell sides by averaging the cell center void fractions of the cells sharing this side. Also, as shown in Eq. (A.3.4), the shear coefficient for a given direction is obtained by multiplying the drag coefficient by the corresponding void fraction. This void fraction has been constrained in the code to be greater than 0.01. TRAC-P1A has no other special treatment for flow orientation.

4.0 Solids to Fluid Momentum Exchange Model

4.1 There is no special treatment of the momentum exchange between the solid boundary and the fluid as a function of flow regime.

4.2 There is no explicit effect of any flow regime on the solid/fluid momentum exchange. The flow regime (based on α) is only used for partitioning the frictional loss to both phases when both exist. This will be explained in Section 4.5.

4.3 TRAC-P1A has two equations of motion for the liquid and the vapor and each of them requires the computation of friction on solid surfaces. The friction terms in these equations are as follows:

$$\frac{C_{w\ell}\, V_\ell \,|V_\ell|}{(1-\alpha)\ \rho_\ell} \quad , \quad \frac{C_{wg}\, V_g \,|V_g|}{\alpha\ \rho_g} \tag{A.4.1}$$

Here $C_{w\ell}$ and C_{wg} are coefficients of friction on the wall. They are related to friction factors C_{fg} and $C_{f\ell}$ obtained from the standard Harwell correlations.

$$C_{w\ell} = (1-\alpha)\ \rho_\ell \ \frac{C_{f\ell}}{2\ D_h} \tag{A.4.2}$$

$$C_{wg} = \alpha\ \rho_g \ \frac{C_{fg}}{2\ D_h} \tag{A.4.3}$$

The Harwell correlation is of proprietary nature and so the details will not be given here. This correlation provides friction factors for co-current two phase mixtures in pipes and goes to correct single phase limits both at $\alpha = 0.0$ and $\alpha = 1.0$. It also has the computations for single phase friction and a two phase multiplier. TRAC-P1A uses it to compute friction factor on solid surfaces for both the phases as shown here

$$C_{f\ell o} = \begin{cases} 0.1 & Re_{\ell o} \le 600 \\ 24/Re_{\ell o} & 600 < Re_{\ell o} < 2000 \\ 0.0055 + 0.40/Re_{\ell o}^{0.333} & Re_{\ell o} \ge 2000 \end{cases} \qquad (A.4.4)$$

$$C_{fg} = C_{f\ell o} \; \phi^2_{\ell o} \qquad (A.4.5)$$

$$C_{f\ell} = C_{f\ell o} \; \phi^2_{\ell o} \qquad (A.4.6)$$

Here $\phi^2_{\ell o}$ is a two phase multiplier and is proprietary. Also notice that the friction factor for all liquid flow, $C_{f\ell o}$, is not continuous at Reynolds number of 600 and 2000. TRAC-P1A also uses this correlation for counter current flow situations by putting the following constraints on the quality calculation in the Harwell correlation

$$\text{for} \quad V_m < 1\,\frac{m}{s}, \quad V^*_m = \text{Max}\left\{1\,\frac{m}{s},\; V_m\right\}, \; G = \rho_m V^*_m \qquad (A.4.7)$$

$$\text{and} \quad x = \rho_g V_g \alpha \,/\, G \qquad (A.4.8)$$

This does not seem to have any basis.

The momentum transfer from the wall to the liquid and to the vapor is partitioned as discussed in Section 4.5. TRAC-P1A has an option of providing additional friction losses at each cell boundary to account for grid spacers and other area changes. However, it does not have any other computation of form losses in the vessel module.

TRAC computes friction losses in the same manner, throughout the vessel in all the directions. However, the code has a slight difference in computing the friction factor in azimuthal direction, where it is based on the velocity on that face, unlike in the other two directions, where the friction factor is based on cell-averaged velocity. It seems that in Equation (A.4.4) TRAC should have 64 instead of 24 for laminar flow range (Re < 2000) and 0.55 instead of 0.40 for the turbulent flow range.

4.4 There is no special model for the area changes in the vessel. The vessel module requires that the area of the side of the cell at which the pipes are connected be equal to the pipe cross sectional area. This eliminates the need of a sudden area change model.

4.5 When there are more than one phase present at the wall, the momentum exchange is partitioned between them. If the void fraction at the wall is less than 0.90, all the momentum exchange is attributed to the liquid phase. However, when the void fraction is between 0.9 and 0.9999, the momentum exchange partition is linearly interpolated. Finally, when the void fraction is greater than 0.9999, all the momentum exchange is with the vapor phase.

$$C_{f\ell} = C_{f\ell(\alpha = 0.9)} \quad (0.9999 - \alpha) \;/\; 0.1 \qquad \alpha > 0.9 \tag{A.4.9}$$

$$C_{fg} = C_{fg(\alpha = 1)} \quad (\alpha - 0.9) \;/\; 0.1 \qquad \alpha > 0.9 \tag{A.4.10}$$

4.6 There is no mechanism to connect the friction coefficient with the wall temperature, other than that it will effect the void fraction, which will in turn change the partition function.

TRAC-P1A uses the HTFS correlation for computing the wall friction coefficient. This correlation was developed for pipes. For radial and azimuthal flow, the fluid is in transverse direction and a pipe flow correlation may not be appropriate. TRAC-P1A also computes flow quality (Equation A.4.8) and restricts the mixture velocity to be greater than 1.0 m/s in the code. This does not seem to have a justification.

5.0 Liquid Entrainment and Deposition

TRAC-P1A has only one model of liquid entrainment to form mist in the annular flow. This model is described by the Wallis correlation and has been coded, as given here.

$$E = 1 - \exp\left[- 0.125\ (J_g' - 1.5)\right] \tag{A.5.1}$$

where

$$J_g' = 10^4\ \alpha\ \frac{V_g\ \mu_g}{\sigma} \left(\rho_g/\rho_\ell\right)^{1/2} \tag{A.5.2}$$

TRAC-P1A also restricts the value of "percent entrainment," E, between 0.07 and 1. However, in the TRAC-P1A documentation, this entrainment correlation is different as shown here,

$$E = 1 - \exp\left[-0.125\,(J_g' - 2.1)\right] \qquad (A.5.3)$$

This correlation is referred to Wallis (1969). However, the above expression could not be found in that reference. It seems that a curve fit for Figure 12.10 of that reference is used. The correlation is a modified form of the Paleev and Filippovich correlation (1966) and is discussed by Wallis (1968) in further detail. The correlation is developed from the air-water data taken at near atmospheric pressure and both the horizontal and vertical tubes of various inside diameters. However, the correlation does not seem to predict the effects of liquid flow rate well (Wallis, 1968). In addition, this correlation may not be appropriate for the flow channels in the vessel, due to cross flow.

6.0 Counter Current Flow Limitation and Liquid Fallback at the Core Support Plates

TRAC vessel model does not have any special formulation or empirical correlations for counter current flow or liquid fall back at the core support plate. However, as the vessel module is based on a two fluid formulation, interfacial shear stress should be able to compute counter current flow situations.

7.0 Energy Transfer Between Liquid and Vapor Fields

7.1 This has been explained in detail in Section A.2.1.

7.2 See Section A.2.1.

7.3 See Section A.2.1.

8.0 Energy Transfer Between Solids (Walls, Internal Structure, Fuel Rods) and Fluid

8.1 TRAC-P1A has the same description of convective heat transfer coefficients for one-dimensional components and the vessel internals. This package includes a boiling curve and the heat transfer correlations for various regions of the boiling curve. These convective heat transfer coefficients are described in detail in part B, Section 8.1. However, in case of reflood, the heat transfer coefficients are different and specialized for the core only. The test for reflood regime is based on core temperature and amount of liquid available. TRAC-P1A first checks the fuel rod temperature to see if the temperature is greater than the

Leidenfrost temperature and then checks if the void fraction is less than 0.995 to ensure the existance of quench front. The Leidenfrost temperature in TRAC is defined as follows

$$T_o = T_s + 100 \text{ (K)} \tag{A.8.1}$$

It would seem that the minimum stable film boiling temperature as described in Section 8.3.2 of Part B would be more appropriate. TRAC-P1A has two methods of reflood, falling film and bottom reflood. In the case of a falling film the heat transfer coefficient for film region is assumed to be a constant as given here

$$h_\ell = 6000 \text{ W/m}^2 \text{ K} \tag{A.8.2}$$

This constant value has not been justified, and from the correlation developed by Yu, Farmer and Coney (1977), it seems that this heat transfer coefficient should be a function of pressure and the Liedenfrost temperature as shown here

$$h_\ell = (F_q/\Delta T_q)^2 \tag{A.8.3}$$

where

$$F_q = 4.52 \text{ X } 10^4 \quad (1 + 0.03\, \Delta T_q\, G_p) \\ (1 + 1.216 \log_{10} p)^{1/2}\; G_p^{\,0.0765/p} \tag{A.8.4}$$

$$\Delta T_q = T_o - T_s \tag{A.8.5}$$

Here G_p is the flow per unit perimeter (kg m^{-1} sec^{-1}) and p is in bar. This correlation was developed for saturated and subcooled water with the test constraints given in Table 4 of Yu, et al (1977). This table is given here again as Table 1.

In the case of bottom reflood, the heat transfer coefficient for the film is computed from the correlation developed by Yu, et al (1977) and is given here

$$h_\ell = (F_q/\Delta T_q)^2 \tag{A.8.6}$$

Table 1

Range of parameters used in the experiments

Test section	Initial dry wall temperatures (°C)	Coolant flowrate (g sec^{-1})	Coolant subcooling (°C)	System pressure (bar)
Falling film experiments Type 321 Stainless steel O.D. 15.9 mm Wall 0.71 mm Length 830 mm	200-650	3-50	0-90	1-14.8
Bottom flooding Type 321 Stainless steel A. O.D. 15 mm Wall 0.71 mm B. O.D. 16.3 mm Wall 1.8 mm Length 1 m approx.	300-800	A. 1-200 B. 2-150	0-70	Atmospheric only

where

$$\Delta T_q = T_o - T_s \tag{A.8.7}$$

$$F_q = \alpha F_s \tag{A.8.8}$$

$$F_s = 4.24 \times 10^4 \, V_\ell \tag{A.8.9}$$

$$\alpha = 0{\cdot}4839 \, (1 + V_\ell \, \Delta T_q^{\,2})^{0.346}, \quad (1 + V_\ell \, \Delta T_q^{\,2}) \geq 40$$

$$ = (1 + V_\ell \, \Delta T_q^{\,2})^{0.13} \qquad (1 + V_\ell \, \Delta T_q^{\,2}) < 40 \tag{A.8.10}$$

This h_ℓ is also restricted to be greater than 6000 W/m^{2}K in TRAC. The data base and the range of experiment is given in Table 4 of Yu, et al., (1977). The liquid velocity in the film is obtained from the cell boundary, as it is one of the variables. [Note that Yu et al., (1977) have suggested a different expression for V_ℓ for tubes as given here:

$$V_\ell = \frac{4 \, M}{\pi \, D^2 \, \rho_\ell} \tag{A.8.11}$$

where M is liquid mass flow rate].

8.2 The heat transfer regimes which are needed for the reactor core under blowdown conditions are described in B.8.1 and for special situations such as reflood, they are discussed in Section A.8.1.

8.3 Selection criteria for these heat transfer regimes are explained in Sections A.8.1 and B.8.1.

8.4 This has been done in Sections A.8.1 and B.8.1.

8.5 The vessel module in TRAC-P1A computes heat transfer coefficient at the solid boundary based on the cell center values. However, it currently computes these coefficients by using only the axial velocities for liquid, vapor and mixture. So there is no special method of computing heat transfer coefficients for flow perpendicular to the fuel rods.

8.6 In situations where liquid and vapor are both at the walls, the heat transfer is shared between the liquid and the vapor phases. TRAC-P1A has two energy equations, vapor energy balance and mixture energy balance. The energy transfered to the liquid and the vapor phases is given by the following expressions,

$$q_{w\ell} = h_{w\ell} \; A_{w\ell} \; (T_w - T_\ell) \; /vol \tag{A.8.12}$$

$$q_{wg} = h_{wg} \; A_{wg} \; (T_w - T_g)/vol \tag{A.8.13}$$

Where $h_{w\ell}$ and h_{wg} are the heat transfer coefficient to the liquid and the vapor phases, while $A_{w\ell}$ and A_{wg} are the portion of the wall area wetted by these phases. In TRAC-P1A, these areas are taken to be equal to the wall areas, i.e.,

$$A_{w\ell} = A_{wg} = A_w \tag{A.8.14}$$

This assumption of using the same areas is good only in nucleate boiling and film boiling regions where convective heat transfer coefficient for one or the other is zero. However, in the transition regime this assumption will overpredict the energy transfer from the wall to the vapor and the liquid.

8.7 TRAC-P1A has the capability to monitor a falling film and the bottom reflood for each of the flow channels. This means that it can handle two quench fronts at the same time. Also, TRAC uses a correlation developed by Dua & Tien (1977) for the quench front velocity as given here.

$$V_{qf} = \frac{k}{\rho c_p \delta} \left[\overline{B} \; (1 + 0.40 \; \overline{B}) \right]^{1/2} \tag{A.8.15}$$

where

$$\overline{B} = B/\overline{T}^2$$

$$B = h_\ell \; \delta / k$$

$$\overline{T} = \theta_o^{\,1/2} \Big/ (1-\theta_o)$$

$$\theta_o = (T_w - T_o) \Big/ (T_w - T_s)$$

and h_ℓ is the film heat transfer coefficient and T_0 is the Leidenfrost temperature, as described in Section A.8.1. Further, δ is the clad thickness and k is the thermal conductivity of clad material.

8.8 TRAC-P1A does not have any special treatment for the grid spacers. However, it does account for the effect of flow reversal on quench front motion. During the bottom reflood, there are two possible situations with flow reversal. In the first situation, the core has low void fraction and an inverted annular flow regime exists. In this case, there is sufficient liquid available in each cell to propagate the quench front. On the other hand, the second situation is connected with high void fraction. In this case TRAC makes a test with the amount of liquid available in each cell, and if sufficient liquid is available, the quench front is propagated, otherwise the quench front velocity is put to zero, and the fuel temperature is computed with a decrease in heat transfer rate. This leads to heating up of the fuel and retreat of the quench front.

B. LIQUID/VAPOR AND FLUID/SOLID INTERACTION IN LOOP COMPONENTS OF TRAC

All the loop components in TRAC are formulated by a five-equation, one-dimensional drift-flux model. The five conservation equations are: Mixture mass, vapor mass, mixture equation of motion, vapor thermal energy and the mixture thermal energy equations. In addition, specifications of relative velocity between the phases, the volumetric phase change rate, vapor-liquid interfacial heat transfer rates, wall shear, and the wall heat transfer are needed. These are supplied by constitutive relations which usually depend on flow regime.

1.0 <u>Flow Regime Recognition Criteria</u>

1.1 There are two different flow-regime maps for the loop components in TRAC-P1A. One is used to calculate the relative velocity between the vapor and the liquid phase, and the other to calculate the interfacial area and heat transfer.

The first flow-regime map, i.e., the map used to determine the flow-regime for relative velocity calculation, is shown in Fig. B.1. Flow-regimes in this map depend both on mixture mass flux and void fraction. There are four transition regions in the map. No particular reason or reference for selecting this map was presented in the TRAC-P1A manual.

The second flow-regime map, i.e., the map used to calculate interfacial area and heat transfer, is the same as used in the Vessel module. See Part A, Section 1.1, for details.

It is worth noting that these two flow-regime maps are not consistent with each other, and there is no apparent reason for using two different maps for the same flow.

1.2 There is no special flow-regime criterion for a specific loop component, pipe orientation or LOCA regime. There is no special treatment for very small break LOCA or natural circulation.

1.3 For the first flow regime, the relative velocity is linearly interpolated with respect to void fraction (for $G < 2000$ kg/m^2-s) in the transition regions. For $2000 < G < 3000$ kg/m^2-s, the relative velocity is linearly interpolated with respect to mass-flux as well as void fraction (if needed).

2.0 <u>Liquid/Vapor Mass Exchange Models and Noncondensible Gas Source/Sink Terms</u>

2.1 The evaporation and condensation models for the loop components are essentially the same as for the vessel module. See Part A, Section 2.1 and 2.2 for details. In loop components the bubble Weber number of 25, (rather than 50 as used in the vessel), and the droplet Weber number of 2 are used.

2.2 No special treatment for individual loop components.

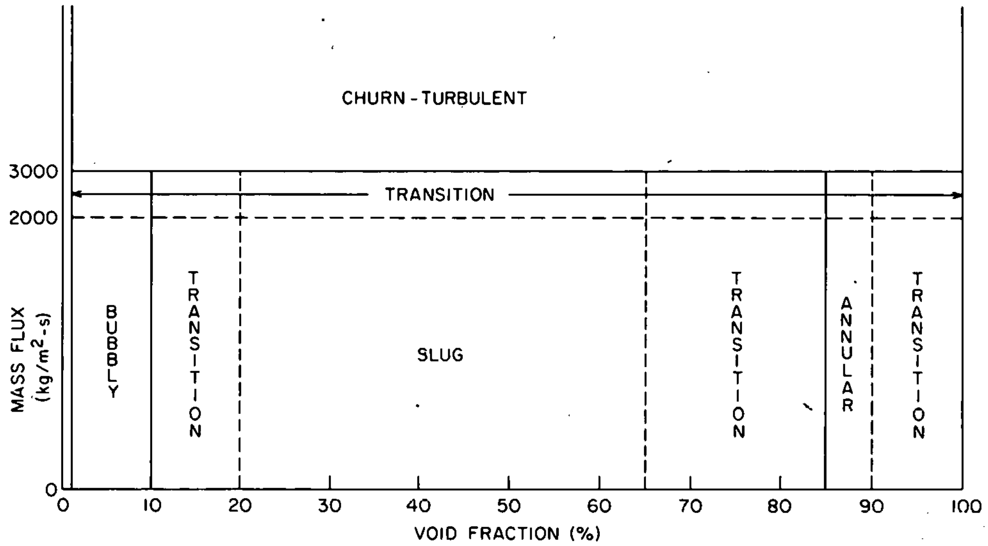

Figure B.1. TRAC flow regime map for slip correlations

2.3 See Part A, Section 2.4.

2.4 TRAC does not handle the effects of embedded solids and walls in liquid/vapor mass exchange models. However, it is well known that embedded solids and wall characteristics influence nucleation, and can affect the rate of phase change.

2.5 TRAC-P1A does not handle the effects of non-condensibles.

2.6 TRAC does not handle nucleation delay. This is a major shortcoming because a number of flashing flow experiments (run at Moby-Dick, BNL, etc.) showed several degrees of liquid superheating at the onset of flashing (or net vapor generation), and it is known that void development can be strongly dependent on this superheat.

2.7 The mass exchange term is calculated from the interfacial energy exchange terms as shown below:

$$\Gamma_v = \frac{-q_{ig} - q_{i\ell}}{h_{fg}} \tag{B.2.1}$$

where Γ_v is the mass rate of vapor generation per unit volume, q_{ig} and $q_{i\ell}$ are the rate of heat transfer per unit volume from interface to vapor and interface to liquid, respectively, and h_{fg} is the latent heat of vaporization.

There is no direct connection between the mass exchange model and the solid/fluid energy exchange model. This is correct in view of the complete nonequilibrium formulation of TRAC.

2.8 There is no model for source/sink of noncondensible gas in TRAC-P1A.

3.0 Liquid/Vapor Momentum Exchange Models

3.1 As the loop components are based on a drift-flux model, rather than a two-fluid model, correlations for relative velocity are specified. For non-horizontal flow, the following correlations are used based on the flow-regime map shown in Fig. B.1. In each case the acceleration due to gravity, g, is an effective value taking into account the orientation of the flow channnel.

(a) Bubbly Regime:

($G \leq 2000$ kg/m^2-s and $0.01 < \alpha \leq 0.1$)

$$V_r = \frac{1.41}{(1 - \alpha)} \left[\frac{\sigma g\ (\rho_\ell - \rho_g)}{\rho_\ell^{\,2}}\right]^{1/4} \tag{B.3.1}$$

(b) Slug Regime:

($G \leq 2000$ kg/m^2-s and $0.2 < \alpha \leq 0.65$)

$$V_r = \frac{0.345}{(1-\alpha)} \left[\frac{gD_h (\rho_\ell - \rho_g)}{\rho_\ell}\right]^{1/2} \tag{B.3.2}$$

(c) Annular Regime:

($G \leq 2000$ kg/m^2-s, and $0.85 < \alpha \leq 0.90$)

$$V_r = \frac{V_m}{\left[\frac{\rho_g (76 - 75\alpha)}{\rho_\ell \sqrt{\alpha}}\right]^{1/2} + \frac{\alpha\rho_g}{\rho_m}} \tag{B.3.3}$$

(d) Churn-Turbulent Regime:

($G \geq 3000$ kg/m^2-s, and for all void fractions)

$$V_r = \frac{V_m}{\frac{(1 - C_o\alpha)}{(C_o - 1)} + \frac{\alpha\rho_g}{\rho_m}} \tag{B.3.4}$$

with $C_o = 1.1$ and α restricted to a maximum value of 0.8. For values of $\alpha > 0.8$, V_r ($\alpha = 0.8$) is used.

(e) for $\alpha \leq 0.005$, $V_r = 0$ (B.3.5)

(f) for $\alpha = 1$, $V_r = 0$ (B.3.6)

(g) Relative velocities in the transition regions (i.e., $0.005 < \alpha \leq 0.01$, $0.1 < \alpha \leq 0.2$, $0.65 < \alpha \leq 0.85$, $0.9 < \alpha \leq 1$ for $G \leq 2000$ kg/m^2-s, and for $2000 < G < 3000$ kg/m^2-s) are linearly interpolated in void fraction and/or mass velocity, G.

The relative velocities for the bubbly and the slug flow regimes are taken from the vapor drift flux correlations presented by Zuber and Findlay (1965). However, the effect of void distribution parameter, C_o, is neglected in TRAC-P1A in these regimes. The correlations, including the effect of void distribution parameter which can range from 1 to 1.6, have been found to agree with experimental data for vertical air-water and steam-water flow systems over a wide range of pressures (up to 40 bar) and pipe diameters (up to 610 mm).

The correlation for annular flow is the simplified version developed by Ishii (1976) and it is valid only for the co-current flows. The data base for the correlation was near-atmospheric tests run in air-water, argon-water and argone-ethyl alcohol vertical upflow systems. The maximum pipe diameter was 32 mm. The gas flow ranged from 150 to 1000 kg/m^2-sec and the liquid flow rate ranged from 200 to 2000 kg/m^2-sec.

In the churn-turbulent regime, TRAC-P1A uses a constant value of 1.1 for the void distribution parameter, C_o. However, an improved correlation (Ishii, 1977) which shows a dependence of C_o on $\sqrt{\rho_g/\rho_\ell}$ is available in the literature. Also, the local drift term is missing from the TRAC formulation of the churn-turbulent regime.

Only in the pressurizer and the accumulator components, a special correlation for drift flux is used (it is not indicated in the TRAC-P1A manual). The correlation as coded is given by

$$V_r = -50[(1 - \alpha_{i-1})\alpha_i]^2 \text{ m/s} \tag{B.3.7}$$

where α_i and α_{i-1} are the cell-centered void fraction above and below the cell boundary where V_r is to be calculated. No reference or justification is given for this correlation.

3.2 Except for the horizontal flow, the gravity term in the different correlations is corrected for the angle between the pipe-axis and a vertical vector pointing upwards, i.e., $g = g_c \cos\Theta$ where g_c is 9.81 m/sec^2.

For horizontal flow ($|g_c \cos\Theta| \leq 10^{-5}$), the relative velocity is calculated by the churn-turbulent correlation (Eq. B.3.4) irrespective of the flow regime.

There is no special treatment for the counter-current flow.

3.3 No step is taken to prevent smearing of the liquid/vapor interface except in the pressurizer and accumulator modules. Special values (Eq. B.3.7) of drift velocities are used in these two latter modules.

4.0 Wall-to-Fluid Momentum Exchange Models

The momentum exchange between the wall and the fluid is expressed through the shear stress at the wall or, in other words, through frictional pressure drop due to the wall. The frictional pressure drop per unit length is written as:

$$\left(\frac{\Delta p}{\Delta X}\right)_f = f_{TP} \frac{2 \rho_m V_m |V_m|}{D_h} \tag{B.4.1}$$

where f_{TP} is the two-phase friction factor, ρ_m is the mixture density, V_m is the mixture velocity and D_h is the hydraulic diameter of the flow channel.

4.1 Except for the accumulator, where the friction factor is set equal to 0.005, the user has six options for calculating friction factors in other loop components. These are:

(i) Constant value (User input)
(ii) Homogeneous model
(iii) Armand correlation
(iv) CISE correlation
(v) Modified annular flow model
(vi) Chisholm correlation

None of the above models/correlations are an explicit function of the flow regime. Therefore, once a particular option is chosen, it is used irrespective of the flow regime. LASL has recommended the homogeneous model for the pressurizer and the steam generator primary and secondary sides. However, no reason is given in the TRAC manual.

We shall now discuss the correlations as they appear in the TRAC-P1A code. Any differences with the manual documentation are noted.

4.1.1 Homogeneous Model

The two-phase friction factor is written as:

$$f_{TP} = f_\ell \, \phi_o^2 \tag{B.4.2}$$

where

$$\phi_o^2 = \left[1 + x\left(\frac{\mu_\ell}{\mu_v} - 1\right)\right]^{-0.2} \tag{B.4.3}$$

and f_ℓ is the single-phase liquid friction factor given by:

$$f_\ell = 0.032 \qquad \text{for } Re_\ell \leq 500 \tag{B.4.4}$$

$$f_\ell = 0.032 - 5.25 \times 10^{-6} (Re_\ell - 500) \qquad \text{for } 500 < Re_\ell < 5000 \tag{B.4.5}$$

$$f_\ell = 0.046 \, Re_\ell^{-0.2} \qquad \text{for } Re_\ell \geq 5000 \tag{B.4.6}$$

$$\text{where } Re_{\ell} \equiv \frac{GD_h}{\mu_{\ell}} \tag{B.4.7}$$

For $Re_{\ell} \geq 5000$, a combination of (B.4.2), (B.4.3) and (B.4.6) yields:

$$f_{TP} = 0.046 \left[\frac{G\ D_h}{\bar{\mu}} \right]^{-0.2} \tag{B.4.8}$$

where

$$\frac{1}{\bar{\mu}} = \frac{x}{\mu_v} + \frac{1-x}{\mu_{\ell}} \tag{B.4.9}$$

The above two equations agree with equations (38) and (39) of TRAC-P1A manual. However, the correlations used for $Re_{\ell} < 5000$, i.e., Eqs. (B.4.4) and (B.4.5), have not been discussed in the manual. It is not clear why the well accepted friction relations for laminar flow have not been used. Even in the turbulent region ($Re_{\ell} \geq 5000$), no data base for using Eq. (B.4.8) is discussed in Ref. 6 (Collier, 1972) of the TRAC manual. It is only mentioned that Eq. (B.4.9) is one way of defining the mixture viscosity.

4.1.2 Armand Correlation

A two-phase multiplier $\phi^2_{\ell o}$ is defined such that

$$\frac{\Delta p_{TP}}{\Delta p_{\ell o}} = \phi^2_{\ell o} \tag{B.4.10}$$

This can be rewritten as:

$$f_{TP} = f_{\ell} \left(\frac{\rho_m}{\rho_{\ell}} \right) \phi^2_{\ell o} \tag{B.4.11}$$

For the single-phase liquid friction factor, Eqs. (B.4.4) through (B.4.7) are used. For the two-phase multiplier, the following correlations are used:

$$\phi^2_{\ell o} = 1 \qquad \text{for } \alpha = 0 \text{ and } \alpha = 1 \tag{B.4.12}$$

$$\phi^2_{\ell o} = (1-x)(1-\alpha)^{-1.42} \qquad \text{for } 0.39 < (1-\alpha) < 1 \qquad (B.4.13)$$

$$\phi^2_{\ell o} = 0.478\ (1-x)^2(1-\alpha)^{-2.2} \qquad \text{for } 0.1 < (1-\alpha) \leq 0.39 \qquad (B.4.14)$$

$$\phi^2_{\ell o} = 1.73\ (1-x)^2\ (1-\alpha)^{-1.64} \qquad \text{for } 0 < (1-\alpha) \leq 0.1 \qquad (B.4.15)$$

Note that Eq. (B.4.11), which is in the code, does not correspond to Eq. (44) of the TRAC manual. Also note that at $\alpha = 1$, i.e., all vapor, the Armand two-phase friction factor as it appears above, does not reduce to the single-phase vapor friction factor. This is a drawback of this correlation.

A check to the original Armand reference as translated by Beak (1959) indicated three mistakes in Equations (B.4.13) through (B.4.15). First, the term (1-x) in Eq. (B.4.13) should be $(1-x)^2$. This is in line with the form of the other equations above. Second, the value 0.39 should be changed to 0.35 in Eqs. (B.4.13) and (B.4.14). Finally, the lower limit of $(1-\alpha)$ in Eq. (B.4.15) should be changed from zero to 0.001. These corrections should be implemented in the future versions of TRAC if the Armand correlation is retained as an option. The Armand correlation has been found to be in good agreement with both air-water data at near atmospheric pressure and steam-water data at higher pressures (3-10 bar). The pipe diameters over which the correlation was tested ranged from 26 mm to 50 mm.

4.1.3 CISE Correlation

The CISE two-phase friction factor as coded in TRAC-P1A reads:

$$f_{TP} = \frac{0.83}{2}\ \rho_m^{-0.46}\ V_m^{-0.6}\ \sigma^{0.4}\ D_h^{-0.2} \qquad (B.4.16)$$

where σ is the surface tension and the units are in S.I. The two-phase friction factor according to (B.4.16) is half of that corresponding to Eq. (45) of TRAC manual.

A check of the reference (Lombardi, 1972) shows that Eq. (B.4.16) is correct. The correlation was obtained from vertical upflow, round tube data, taken with different two-phase mixtures (steam-water, argon-water, nitrogen-water and argon-ethyl alcohol) and covered the following range:

$5 < D < 25$mm

$100 < L < 4000$ mm

$500 < G < 5000\ kg/m^2 - s$

$20 \times 10^{-3} < \sigma < 80 \times 10^{-3}$ N/m

$0.01 < x < 0.98$

$15 < \rho_\ell/\rho_g < 100$

(or, $20 < p < 90$ bar for steam-water mixture.)

It should be noted that the correlation does not reduce to single-phase friction factor values at either x=0 or x=1. This is a major limitation of the correlation. Besides, it is important to recognize that dimensional correlations like (B.4.16) are not generally amenable to extrapolation and should not be used outside the range of their data base.

4.1.4 Annular Flow Model

The two-phase friction factor according to this model and as coded in TRAC-P1A is:

$$f_{TP} = f_{sp\ell} \frac{\rho_\ell V_\ell^2}{\rho_m V_m^2} \qquad (\alpha \leq 0.9) \qquad \text{(B.4.17)}$$

where the single-phase liquid friction factor is taken as (Govier and Aziz, 1972):

$$f_{sp\ell} = a + b\ Re^{-c} \qquad \text{(B.4.18)}$$

and

$$a = 0.026 \left(\frac{k}{D_h}\right)^{0.225} + 0.133\ \frac{k}{D_h} \qquad \text{(B.4.19)}$$

$$b = 22.0 \left(\frac{k}{D_h}\right)^{0.44} \qquad \text{(B.4.20)}$$

$$c = 1.62 \left(\frac{k}{D_h}\right)^{0.134} \qquad \text{(B.4.21)}$$

$$Re = \frac{\rho_\ell V_\ell D_h}{\mu_\ell} \qquad \text{(B.4.22)}$$

(k/D_h) is the roughness factor. A value of $k = 5.0 \times 10^{-6}$m is used in the code. Note that Eq. (B.4.18) does not reduce to the smooth-wall friction factor for $(k/D_h) \rightarrow 0$, and a certain amount of roughness ($k/D_h \approx 10^{-6}$) has to be specified even for smooth pipes.

For $\alpha > 0.9995$, the homogenous friction factor as discussed in Section 4.1.1 is used. In between, i.e., $0.9 < \alpha \leq 0.9995$, a linear interpolation between the annular flow model and the homogenous model is used.

It should be noted that there is a discrepancy between Eq. (B.4.17) and Eqs. (50)-(51) of TRAC-P1A manual. Moreover, Eq. (B.4.17) is only valid for annular flow with negligible flow quality, i.e., $x \approx 0$. Also, the exponent 0.134 is missing from Eq. (69) of the TRAC manual.

4.1.5 Chisholm Correlation

This correlation is also based on the two-phase multiplier $\phi^2_{\ell o}$ as defined in (B.4.10). The correlation is written as:

$$f_{TP} = f_{sp\ell} \left(\frac{\rho_m}{\rho_\ell}\right) \phi^2_{\ell o} \qquad \text{(B.4.23)}$$

The single phase friction factor is calculated from Eqs. (B.4.18) through (B.4.21) with $k = 5.0 \times 10^{-6}$m. The definition of liquid Reynolds number is, however, GD_h/μ_ℓ and differs from Eq. (B.4.22). The Chisholm two-phase multiplier is given by:

$$\phi^2_{\ell o} = 1 + (R^2 - 1)\ [Bx\ (1 - x) + x^2] \qquad \text{(B.4.24)}$$

where $\quad R = (\rho_\ell/\rho_g)^{0.5} \quad$ (for rough tubes).

The values for B are given in Eqs. (54) through (56) in the TRAC manual.

It should be noted that for a smooth pipe the use of $R = (\rho_\ell/\rho_g)^{0.5}$, leads to the problem of $f_{TP} \neq f_g$ for $x = 1$. In that case, the complete form of the Chisholm correlation (Chisholm, 1973) with $R \equiv \left(\Delta p_{go}/\Delta p_{\ell o}\right)^{0.5} = (\rho_\ell/\rho_g)^{0.5} (\mu_g/\mu_\ell)^{n/2}$ should have been used (but it is not in TRAC). The data base for this correlation includes steam-water mixtures at $300 < G < 7000$ kg/m^2-s, $6 < p < 140$ bar and $0.015 < x < 0.8$. Maximum hydraulic diameter was 27 mm.

4.2 The TRAC code has two different treatments for form losses due to abrupt expansion or contraction. If the system of equations is solved implicitly, i.e., IHYDRO = 1, the additional pressure drop due to expansion and contractions are given by:

For Expansion:

$$\Delta p = \frac{1}{2} \left(1 - \frac{A_1}{A_2}\right)^2 \rho_m V_m^2 \tag{B.4.25}$$

and, for Contraction:

$$\Delta p = \frac{1}{2} \left[0.5 - 0.7 \frac{A_1}{A_2} + 0.2 \left(\frac{A_1}{A_2}\right)^2 \right] \rho_m V_m^2 \tag{B.4.26}$$

where A_1 and A_2 are the smaller and the larger flow areas, respectively. In the code, however, the switch from the expansion equation to the contraction equation and vice-versa is done at area ratio of 0.9 instead of 1.0. This seems to be an oversight.

For the semi-implicit solution scheme, i.e., IHYDRO = 0, LASL states (but it could not be verified at BNL at the time of this writing) that the spatial differencing scheme by itself takes care of the form loss due to abrupt expansion. Therefore, the form loss term for expansion is set to zero. However, extra terms are added for a transition region and abrupt contraction. They are as follows:

(a) Transition Region $\left(0.9 < \frac{A_+}{A_-} < 1.1\right)$

$$\Delta p_{extra} = 1/2\ \rho_m V_m^2 \left[\frac{\Delta X_- - \Delta X_+}{\Delta X_-} \left(1 - \frac{A_f}{A_-}\right) - \left(1 - \frac{A_f}{A_-}\right)^2\right] \tag{B.4.27}$$

where A_-, A_+ and A_f are the cross-sectional area of the upstream, downstream and the minimum flow area, respectively. ΔX_- and ΔX_+ are the cell lengths at the upstream and downstream, respectively.

(b) Abrupt Contraction $\left(\frac{A_+}{A_-} \leq 0.9\right)$

$$\Delta p_{extra} = 1/2\ \rho_m V_m^2 \left[\frac{\Delta X_- - \Delta X_+}{\Delta X_-} \left(1 - \frac{A_f}{A_-}\right) - \left\{0.5 - 1.3 \frac{A_f}{A_-} + 0.8 \left(\frac{A_f}{A_-}\right)^2\right\}\right] \tag{B.4.28}$$

The reasons for having a transition region and the term $\frac{\Delta X_- - \Delta X_+}{\Delta X_-}\left(1 - \frac{A_f}{A_-}\right)$ is not clear. If it is ignored and we assume that the term $\frac{1}{2} \rho_m V_m^2 \left(1 - A_f/A_-\right)^2$ is added through the difference equation, then Eq. (B.4.28) does correspond to Eq. (B.4.26) for abrupt contraction.

4.3 There is no special treatment for void fraction distribution in a TEE branch or in the steam generator tubes. Also, there is no separate model for the TEE component which is basically a combination of two PIPE components.

4.4 For loop components there is only one momentum equation, i.e., the mixture momentum, per cell. Therefore, there is no question of partitioning the wall-to-fluid momentum exchange.

5.0 <u>Liquid Entrainment and Deposition Models</u>

Same as Section 5.0 in Part A.

6.0 <u>Counter-Current Flow Limitation</u>

There is no special model (or drift velocity) to account for the counter-current flow limitation.

7.0 <u>Models for Energy Transfer Between Liquid & Vapor</u>

Same as Section 7.0 in Part A.

8.0 <u>Energy Transfer Between Solids (Walls) and Fluid</u>

8.1 Based on the local surface (wall) temperature, surface properties and fluid conditions, the heat transfer coefficients between the wall and the fluid (liquid and vapor) are calculated from a generalized boiling curve. This is shown in Figure B.2. Four different heat transfer regimes are shown in the above figure. These are:

(a) Convective heat transfer to single phase liquid (i=1)

(b) Nucleate boiling and forced convection vaporization (i=2)

(c) Transition boiling (i=3)

(d) Film boiling (i=4)

There are several other heat transfer regimes not shown in the boiling curve. These are:

(e) Free or forced convection to vapor, when $\alpha \geq 0.9995$ (i=6)

(f) Forced convection to mixture, when CHF calculation is not asked for, i.e., ICHF=0 (i=7)

(g) Horizontal film condensation (i=11)

(h) Vertical film condensation (i=12)

(i) Turbulent film condensation (i=13)

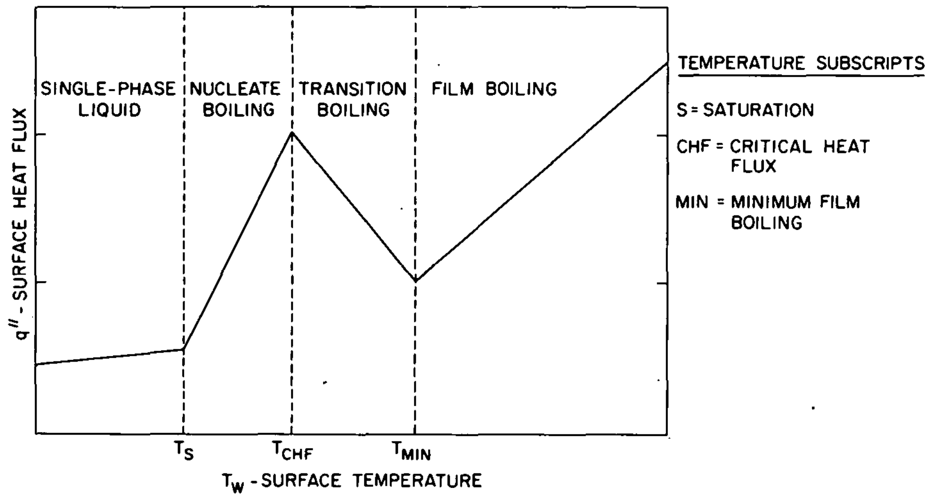

Figure B.2. Generalized boiling curve

8.2 The same heat transfer subroutine HTCOR is called by all the components, including the steam generator primary and secondary side and the vessel module. Therefore, there is no special treatment for heat transfer in any particular component.

8.3 The selection logic to identify different heat transfer regimes is depicted in Figure B.3. There are two important surface temperatures--namely, the temperature at Critical Heat Flux and temperature at Minimum Stable Film Boiling which determine the boundaries between the nucleate boiling (i=2), transition boiling (i=3) and the film boiling (i=4) regimes and these need further discussion. (There is no special selection criteria for Steam generator secondary side).

8.3.1 Surface Temperature at Critical Heat Flux

Based on the local fluid conditions, the critical heat flux is calculated either by the modified Zuber pool boiling correlation, or Biasi, et al. correlation or by the Bowring correlation. The Chen correlation for the nucleate boiling heat transfer coefficient is then used to calculate the surface temperature corresponding to the critical heat flux such that:

$$T_{CHF} = T_{sat} + \frac{q''_{CHF}}{h_{CHEN}} \qquad (B.8.1)$$

In the code, however, T_{CHF} is restricted between T_{sat} + 5°K and T_{sat} + 100°K.

The modified Zuber correlation for pool boiling CHF is used for $-600 < G < 100$ kg/m^2-sec. This is in line with the recommendation of Bjornard and Griffith (1977). However, they suggested a multiplier 0.9 for vertical rod geometry in the modified Zuber correlation, which is missing in TRAC formulation. In TRAC-P1A code, a correction term for subcooled CHF has been added. But it is not reported in the TRAC manual. The modified Zuber correlation as appears in the code reads:

$$q''_{CHF} = (1-\alpha)\left[0.131\,\rho_g\,h_{fg}\left\{\frac{\sigma g\left(\rho_\ell-\rho_g\right)}{\rho_g^2}\right\}^{1/4} + 0.696\sqrt{k_\ell \rho_\ell c_{p\ell}}\left\{\frac{g\left(\rho_\ell-\rho_g\right)}{\sigma}\right\}^{1/4}\left\{\frac{\sigma g\left(\rho_\ell-\rho_g\right)}{\rho_g^2}\right\}^{1/8}\left(T_{sat}-T_\ell\right)\right] \qquad (B.8.2)$$

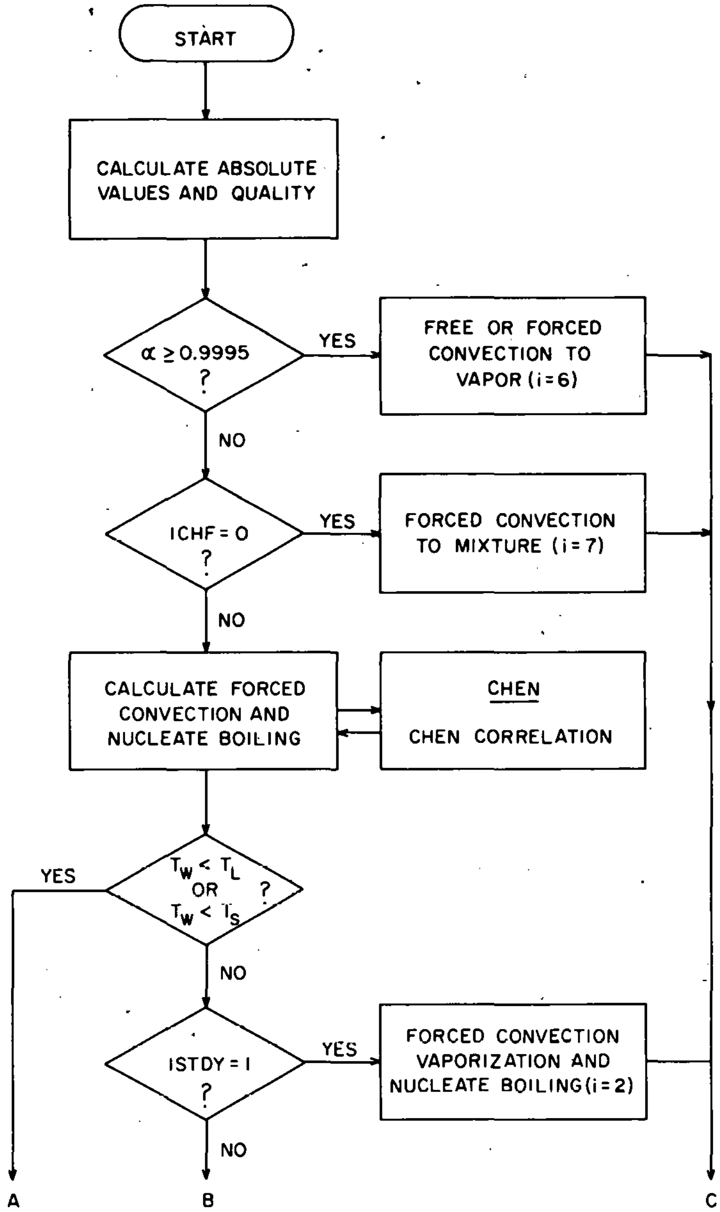

Figure B.3. Heat transfer regime and correlation selection logic

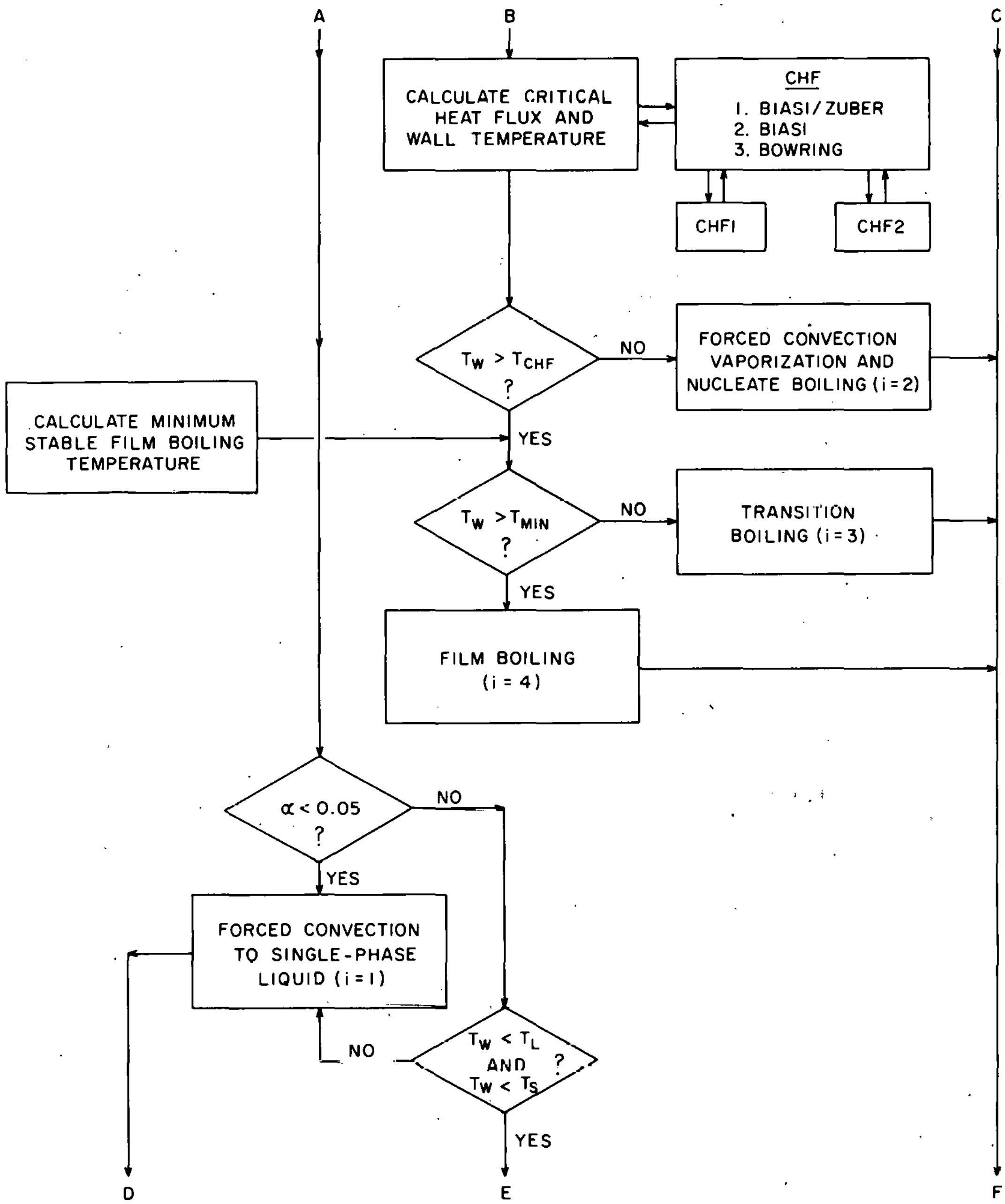

Figure B.3. (Continued) Heat Transfer regime and correlation selection logic

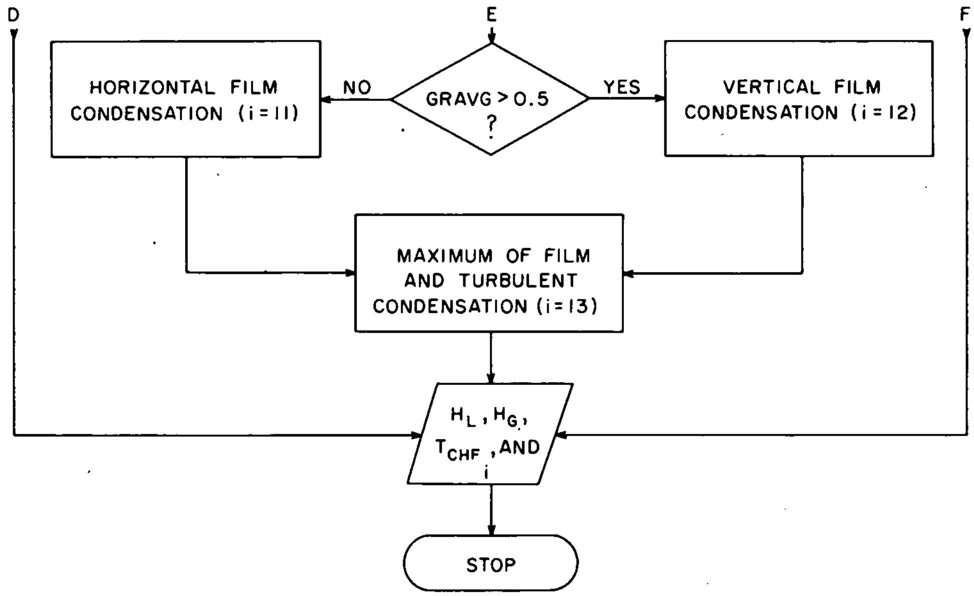

ICHF = CHF TEST FLAG
ISTDY = STEADY STATE FLAG
GRAVG = g cos θ

Figure B.3. (Continued) Heat transfer regime and correlation selection logic

For high flow rates, i.e., $G > 200\ kg/m^2$-sec. and $G < -700\ kg/m^2$-sec., the Biasi, et al. (1967) correlation is used. The correlation is described by Eqs. (127) and (128) of TRAC-P1A manual and will not be repeated here. (There are a few typographical errors in the manual and one error in the code, which has been corrected by LASL recently). The Biasi correlation has been developed from steam-water critical heat flux data taken in round tubes with uniform heat flux, and the range of validity is:

$3 < D < 37.5$ mm

$200 < L < 6000$ mm

$2.7 < p < 140$ bar

$100 < G < 6000\ kg/m^2$-sec.

$x_{in} < 0$

$$\frac{1}{1 + \rho_\ell/\rho_g} < x_{out} < 1$$

In the intermediate range of mass flux, i.e., $100 < G < 200\ kg/m^2$-sec and $-700 < G < -600\ kg/m^2$-sec, a linear interpolation between $q''_{CHF,ZUBER}$ and $q''_{CHF,BIASI}$ is done. No particular reason for using the Biasi correlation is given.

For loop components, i.e., the one-dimensional formulation, the Bowring correlation, based on round tubes and uniform heat flux data, is available to the user by setting ICHF = 3.

The original Bowring correlation (Bowring, 1972) was of the form:

$$q''_{CHF} = (A + B\ H_i)/(C + L) \qquad \text{(B.8.3)}$$

where H_i and L were the inlet subcooling and the tube length, respectively. LASL, however, has modified the above form and used the following:

$$q''_{CHF} = (A - B\ h_{fg}\ x)/C \qquad \text{(B.8.4)}$$

where x is the local flow quality. This modification is valid only for round tubes and uniform heat flux situations.

The data base for (B.8.3) or (B.8.4) was:

$2 < D < 45$ mm

$150 < L < 3700$ mm

$7 < p < 170$ bar

$136 < G < 18600\ kg/m^2$-s

The coefficients A, B, and C are complicated functions of pressure, mass flux and diameter, and are given in the TRAC manual. They will not be repeated here. However, the definition of p_R as given in the TRAC manual is incorrect. It should be $p_R = 0.145\ p/10^6$. It has been coded correctly.

8.3.2 Surface Temperature at Minimum Stable Film Boiling

This temperature determines the boundary between the transition boiling regime and the film boiling regime. In TRAC, the homogeneous nucleation mechanism has been assumed to govern the minimum temperature as per recommendation of Bjornard and Griffith (1977). Therefore, T_{min} is given by:

$$T_{min} = T_{HN} + \left(T_{HN} - T_\ell\right) \frac{\left[k_\ell \rho_\ell c_{p\ell}\right]^{1/2}}{\left[k_w \rho_w c_{pw}\right]^{1/2}} \tag{B.8.5}$$

For simplicity, the homogeneous nucleation temperature, T_{HN}, in TRAC is taken to be equal to the thermodynamic critical temperature of the fluid, T_{crit}. The subscript w stands for wall material properties which depend on the surface condition, i.e., oxidation, crud formation, aging, etc. However, these effects are not included in TRAC at present.

8.4 Heat Transfer Correlations

8.4.1 Convective Heat Transfer to Single Phase Liquid (i=1):

The maximum of the following laminar and the turbulent (Dittus-Boelter) correlation is used.

$$h_{\ell,laminar} = 4 \frac{k_\ell}{D} \tag{B.8.6}$$

and

$$h_{\ell,turbulent} = 0.023 \frac{k_\ell}{D} Re_\ell^{0.8} Pr_\ell^{0.4} \tag{B.8.7}$$

8.4.2 Nucleate Boiling and Forced Convection Vaporization (i=2):

The widely accepted Chen correlation is used in this regime. The correlation has been developed from data taken in round tubes and annuli with water and several different organic fluids. Both upflow and downflow data were used. The range of data used include:

$0.55 < p < 35$ bar

$0.06 < V_{\ell,in} < 4.5$ m/s

$0.01 < x < 0.59$

$6.2 < q''_w < 2400$ kW/m^2

The correlation has been described in Eq. (137) of the TRAC-P1A manual and will not be repeated here.

For $\alpha < 0.995$, the heat transfer coefficients between the wall and the liquid, h_ℓ, and the vapor, h_v, are given by:

$$h_\ell = h_{CHEN}$$

$$h_v = 0$$

whereas, for $0.995 \leq \alpha \leq 0.9995$

$$h_\ell = \left[1 - \frac{(\alpha - 0.995)}{0.0045}\right] h_{CHEN}$$

$$h_v = \frac{(\alpha - 0.995)}{0.0045} \text{ Max} \left\{ h_{v,nc} \quad , \quad h_{v,turbulent} \right\}$$

where, $h_{v,nc}$ and $h_{v,turbulent}$ are described in Section 8.4.5.

8.4.3 Transition Boiling (i=3):

Heat transfer to the liquid, in this regime, is comprised of three components--namely, the transition boiling heat transfer, radiative heat transfer to liquid and heat transfer to subcooled liquid (which is not documented in the TRAC-P1A manual). The transition boiling component is given by (following the approach of Bjornard and Griffith, 1977).

$$h_{TB} = \left[\delta\, q''_{CHF} + (1 - \delta)\, q''_{min}\right] \Big/ \left(T_w - T_{sat}\right) \tag{B.8.8}$$

where

$$\delta = \left(\frac{T_w - T_{min}}{T_{CHF} - T_{min}}\right)^2 \tag{B.8.9}$$

and $q''_{min} = (1 - \alpha)\, h_{FB}\, (T_{min} - T_{sat})$ (B.8.10)

The film boiling heat transfer coefficient, h_{FB}, is calculated from the modified Bromley correlation and is given by:

$$h_{FB} = 0.62 \left[\frac{k_g^3 \left(\rho_\ell - \rho_g\right) g\, h'_{fg}}{\mu_g \left(T_w - T_{sat}\right) \lambda} \right]^{1/4} \qquad \text{(B.8.11)}$$

where $h'_{fg} = h_{fg} + 0.5\, c_{p,g}\, (T_w - T_{sat})$ (B.8.12)

and $$\lambda = 2\pi \left[\frac{\sigma}{g \left(\rho_\ell - \rho_g\right)} \right]^{1/2} \qquad \text{(B.8.13)}$$

The radiative component to liquid is given by:

$$h_{RAD} = \sigma_s\, F \left(T_w^4 - T_\ell^4\right) \Big/ \left(T_w - T_\ell\right) \qquad \text{(B.8.14)}$$

where σ_s = Stefan-Boltzman Constant = 5.6697×10^{-8} W/m^2-K^4

and $$F = \frac{1}{\frac{1}{\varepsilon} + \frac{1}{a} - 1} \qquad \text{(B.8.15)}$$

where ε = emissivity of the wall
a = absorptivity of the liquid

For subcooled liquid, the code has an additional heat transfer component to liquid (Linehan and Grolmes, 1970), but not reported in the TRAC manual:

$$h_{\ell,sc} = 0.012\, \rho_\ell\, c_{p,\ell}\, V_\ell \qquad \text{(B.8.16)}$$

Therefore, the heat transfer coefficient to liquid in the transition region is given by:

$$h_\ell = h_{TB} + \frac{T_w - T_{CHF}}{T_{min} - T_{CHF}} (1 - \alpha) \left\{ h_{RAD} + h_{\ell,sc} \frac{\left(T_s - T_\ell\right)}{\left(T_w - T_\ell\right)} \right\} \qquad \text{(B.8.17)}$$

The vapor heat transfer coefficient is given by:

$$h_v = \alpha \frac{\left(T_w - T_{CHF}\right)}{\left(T_{min} - T_{CHF}\right)} \quad \text{Max} \left\{ h_{v,nc} \ , \ h_{v,DR} \right\} \tag{B.8.18}$$

$h_{v,DR}$ is the Dougall-Rohsenow heat transfer coefficient and discussed next.

8.4.4 Film Boiling (i=4):

The liquid and vapor heat transfer coefficients in this regime are given by:

$$h_\ell = (1 - \alpha) \left[h_{RAD} + h_{\ell,sc} \frac{\left(T_s - T_\ell\right)}{\left(T_w - T_\ell\right)} \right] \tag{B.8.19}$$

where h_{RAD} and $h_{\ell,sc}$ are given by Eqs. (B.8.14) and (B.8.16), respectively.

$$h_v = (1 - \alpha) \frac{\left(T_w - T_{sat}\right)}{\left(T_w - T_v\right)} h_{FB} + \alpha \text{ Max} \left\{ h_{v,nc}, \ h_{v,DR} \right\} \tag{B.8.20}$$

where h_{FB} is given by (B.8.11), $h_{v,nc}$ is discussed in Section 8.4.5 and $h_{v,DR}$ is the Dougall-Rohsenow correlation expressed as:

$$h_{v,DR} = 0.023 \frac{k_g}{D} \left\{ \frac{\rho_g \left[\alpha V_g + (1 - \alpha) V_\ell \right] D}{\mu_g} \right\}^{0.8} Pr_g^{0.4} \tag{B.8.21}$$

Although not mentioned in the TRAC manual, LASL indicated that the form of Eq. (B.8.20) has been adopted following recommendation of Dr. Y. Y. Hsu of USNRC.

8.4.5 Free or Forced Convection to Vapor (i=6):

When $\alpha \geq 0.9995$ and for calculating vapor heat transfer coefficient for transition and film boiling, the free convection heat transfer to vapor is calculated as (following McAdams):

$$h_{v,nc} = 0.13 \frac{k_g}{D} \left[\frac{D^3 \rho_g^2 g \left(T_w - T_v\right)}{\mu_g^2 \, T_v} \right]^{1/3} Pr_v^{1/3} \tag{B.8.22}$$

Note that the characteristic dimension does not have any effect in the above equation. The turbulent forced convection heat transfer is then calculated from the Dittus-Boelter correlation:

$$h_{v,\ turbulent} = 0.023 \frac{k_g}{D} Re_v^{0.8} \; Pr_v^{1/3} \tag{B.8.23}$$

The maximum of $h_{v,nc}$ and $h_{v,turbulent}$ is chosen for h_v, whereas h_ℓ is set to zero.

8.4.6 Forced Convection to Two-Phase Mixture (i=7):

When ICHF=0, i.e., the critical heat flux calculation is not asked for by the user, TRAC calculates heat transfer to two-phase mixtures in the following manner:

For $\alpha \leq 0.995$,

$$h_v = 0 \tag{B.8.24}$$

$$h_\ell = \text{Max} \left\{ h_{\ell,LAM}, h_{\ell,turb} \right\} \tag{B.8.25}$$

where $h_{\ell,LAM} = 4 \frac{k_\ell}{D}$ (B.8.26)

and $$h_{\ell,\ turb} = 0.023 \frac{k_g}{D} \left(\frac{GD}{\mu_m}\right)^{0.8} Pr_\ell^{0.4} \tag{B.8.27}$$

where $$\mu_m \equiv \frac{1}{\frac{x}{\mu_g} + \frac{1-x}{\mu_\ell}} \tag{B.8.28}$$

Note that the TRAC manual refers to a two-phase thermal conductivity which is not, in fact, used in the code. The documentation reference to Dittus-Boelter is, of course, only with reference to the form of the correlation as applicable to single-phase flow. The form used herein can be considered as application of Reynolds analogy to the momentum exchange expressed by Eqs. B.4.8 and B.4.9. The validity of Eq. (B.8.27) for two-phase application could not be checked with experimental data due to lack of proper reference.

For $0.995 < \alpha \leq 0.9995$

$$h_v = \frac{\alpha - 0.995}{0.0045} \text{ Max } \left\{ h_{v,nc}, h_{v,\text{ turbulent}} \right\} \tag{B.8.29}$$

and
$$h_\ell = \left[1 - \frac{(\alpha - 0.995)}{0.0045} \right] \text{ Max } \left\{ h_{\ell,LAM}, h_{\ell,turb} \right\} \tag{B.8.30}$$

8.4.7 <u>Condensation Regimes (i=11,12,13)</u>:

If the surface temperature is less than both the liquid temperature and the saturation temperature, the TRAC heat transfer logic chooses the condensation regimes. First, the laminar film condensation heat transfer is calculated in the following way:

For $g_c \cos\Theta \leq 0.5$, $(\Theta > 87.1^o)$, film condensation in horizontal pipe Chato, 1962) is selected (i=11):

$$h_{\ell,Hor} = 0.296 \left[\frac{\rho_\ell \left(\rho_\ell - \rho_g\right) g\, h_{fg}\, k_\ell^3}{D\mu_\ell \left(T_{sat} - T_w\right)} \right]^{1/4} \tag{B.8.31}$$

For $g_c \cos\Theta > 0.5$, i.e., vertical film condensation, TRAC uses the following Nusslet type correlation (i=12):

$$h_{\ell,Ver} = 1.132 \left[\frac{\rho_\ell \left(\rho_\ell - \rho_g\right) g \cos\Theta\, h_{fg}\, k_\ell^3}{D\mu_\ell \left(T_{sat} - T_w\right)} \right]^{1/4} \tag{B.8.32}$$

The coefficient 1.132 is obtained by multiplying the original Nusselt coefficient of 0.943 by 1.2 to account for the waviness of the film. However, in the original Nusselt formulation, the characteristic dimension was the axial length and not the pipe diameter. No reference, which could support this change in characteristic dimension, was given.

The correlation of Carpenter and Colburn (1951) for turbulent film condensation is then calculated in the following way (i=13):

$$h_{\ell,\text{ turb}} = 0.065 \frac{k_\ell \rho_\ell^{1/2}}{\mu_\ell} Pr_\ell^{1/2} \tau_i^{1/2} \tag{B.8.33}$$

where τ_i, the interfacial friction factor is assumed to be the same as the wall friction factor for vapor flow only and is given by

$$\tau_i = 0.046 \left(\frac{\rho_g V_g D}{\mu_g}\right)^{-0.2} \frac{\rho_g V_g^2}{2} \qquad \text{(B.8.34)}$$

Eq. (B.8.33) has been found to be the average heat transfer coefficient for condensation of pure vapor of various fluids (water, methanol, ethanol, toluene and trichlorethylene) in a 12 mm ID, 2440 mm long vertical pipe with inlet vapor velocities up to 150 m/sec.

The heat transfer coefficient to liquid is then taken as

$$h_\ell = \text{Max} \left\{ h_{\ell,\text{turb}},\ h_{\ell,\text{Hor}} \text{ or } h_{\ell,\text{Ver}} \right\} \qquad \text{(B.8.35)}$$

8.5 In the flow regimes where both the liquid and vapor heat transfer coefficients are non-zero, TRAC uses the same heated surface area for both parts. That is to say that:

$$q_{wg} = h_{wg}\, A\, (T_w - T_g)/\text{vol} \qquad \text{(B.8.36)}$$

$$q_{w\ell} = h_{w\ell}\, A\, (T_w - T_\ell)/\text{vol} \qquad \text{(B.8.37)}$$

where A is the actual heated surface area in a computational cell. As mentioned in Section 8.6 of Part A, this assumption will overpredict the energy transfer from the wall to the fluid for the transition boiling regime.

REFERENCES

Akagawa, K., and Sakaguchi, T., (1966), Bulletin J.S.M.E., 9, p. 104.

Beak, V. (1959), "The Resistance During the Movement of a Two-Phase System in Horizontal Pipes," by A. A. Armand, AERE Trans. 828.

Biasi, L., et. al., (1967), "Studies on Burnout - Part 3," Energia Nucleare, Vol. 14, No. 9, pp. 530-536.

Bjornard, T. A. and Griffith, P., (1977), "PWR Blowdown Heat Transfer," in Thermal and Hydraulic Aspects of Nuclear Reactor Safety, Vol. 1 (American Society of Mechanical Engineers, New York 1977), pp. 17-41.

Bowring, R. W., (1972), "A Simple But Accurate Round Tube, Uniform Heat Flux Dryout Correlation over the Pressure Range 0.7-17 MN/m^2 (100-2500 psia)," Atomic Energy Establishment report AEEW-R789.

Carpenter, E. F. and Colburn, A. P., (1951), "The Effect of Vapor Velocity on Condensation Inside Tubes," Proceedings of the General Discussion on Heat Transfer, The Inst. of Mech. Engineers and the ASME, pp. 20-26.

Chato, J. C., (1962), "Laminar Condensation Inside Horizontal and Inclined Tubes," A.S.H.R.A.E. Journal 4, pp. 52-60.

Chisolm, D., (1973), "Pressure Grandients Due to Friction During the Flow of Evaporating Two-Phase Mixtures in Smooth Tubes and Channels, " Int. J. Heat Mass Transfer 16, pp. 347-358.

Collier, J. G., (1972), "Convective Boiling and Condensation" (McGraw-Hill Co., New York).

Dua, S. S. and Tien, C. L., (1977), "Generalized Two-Parameter Relation for Conduction-Controlled Rewetting of a Hot Vertical Surface," International Journal of Heat and Mass Transfer, 20, pp. 174-176.

Govier, G. W. and Aziz. A., (1972), "The Flow of Complex Mixtures in Pipes" (Van Nostrand-Rheinhold Co., New York).

Ishii, M., (1976), "Light-Water-Reactor Research Program," Argonne National Laboratory report ANL77-10 (Oct.-Dec. 1976).

Ishii, M., (1977), "One-Dimensional Drift-Flux Model and Constitutive Equations for Relative Motion Between Phases in Various Two-Phase Flow Regimes," ANL-77-47.

Lee, K. and Ryley, D. J., (1968), "The Evaporation of Water Droplets in Superheated Steam," Journal of Heat Transfer, Nov. 1968, pp. 445-451.

Lekach, S. (1975), "Development of a Computer Code for Thermal Hydraulics of Reactors (THOR)," Brookhaven National Laboratory Quarterly Progress Report, BNL-19978.

Linehan, J. H. (1968), "The Interaction of Two-Dimensional Stratified, Turbulent Air-Water and Steam-Water Flows," ANL-7444, May 1968.

Linehan, J. H. and Grolmes, M. A., (1970), "Condensation of a High Velocity Vapor on a Subcooled Liquid Jet in Stratified Flow," Proceedings of the 4th Int. Heat Transfer Conference, Paper No. Cs 2.6, Paris.

Lombardi, C., and Pedrocchi, E., (1972), "A Pressure Drop Correlation in Two-Phase Flow," Energia Nucleare, Vol. 19, No. 2. pp. 91-99.

Paleev, I. I. and Filippovich, B. S., (1966), "Phenomena of Liquid Transfer in Two-Phase Dispersed Annular Flow," Int. J. of Heat and Mass Transfer, Vol. 9, pp. 1089-1093.

Plesset, M. S. and Zwick, S. A. (1954), "The Growth of Vapor Bubbles in Superheated Liquids," Journal of Applied Physics, Vol. 25, Number 4, p. 493.

"TRAC-P1A: An Advanced Best-Estimate Computer Program for PWR LOCA Analysis," (May 1979), Los Alamos Scientific Laboratory Report LA-7777-MS, NUREG/CR-0665.

Wallis, G. B., (1968), "Phenomena of Liquid Transfer in Two-Phase Dispersed Annular Flow," Int. J. of Heat and Mass Transfer, Vol. 11, pp. 783-785.

Wallis, G. B., (1969), "One-Dimensional Two-Phase Flow," McGraw Hill, N.Y.

Wallis, G. B., (1970), "Annular Two-Phase Flow, Part 1, A Simple Theory," Journal of Basic Engineering, ASME, March 1970, pp. 59-72.

Yu, S. K. W., Farmer, P. R., and Coney, M. W. E., (1977), "Methods and Correlations for the Prediction of Quenching Rates on Hot Surfaces," International Journal of Multiphase Flow, Vol. 3, pp. 415-443.

Zuber, N. and Findlay, J. A., (1965), "Average Volumetric Concentrations in Two-Phase Flow Systems," J. Heat Trans. 87, p. 453.

DISTRIBUTION

BNL NSP Division Heads
BNL NSP Group Leaders
BNL RSE Personnel
TRAC Assessment Group
W. D. Beckner, NRC
S. Fabic, NRC
Y. Y. Hsu, NRC
J. Jackson, LASL
W. Y. Kato, BNL
H.J.C. Kouts, BNL
F. Odar, NRC
R. Scroggins, NRC
L. Shotkin, NRC
L. H. Sullivan, NRC
L. S. Tong, NRC
N. Zuber, NRC